PLY-THICKNESS AND PLY-BLOCK EFFECT ON FIBER/MATRIX INTERFACE CRACK GROWTH IN CROSS-PLY LAMINATES UNDER TENSILE LOADING

INSIGHTS FROM LEFM-BASED MICROMECHANICAL MODELING

L. Di Stasio[1,2]

[1] Division of Materials Science, Luleå University of Technology, Luleå, Sweden
[2] EEIGM & IJL, Université de Lorraine, Nancy, France

Instituto IMDEA Materiales

Getafe, Madrid (ES) - September 17, 2019

Outline

- Transverse Cracks Initiation
- Modeling
- Debond Initiation
- Debond Propagation
- Conclusions

↘ TRANSVERSE CRACKS INITIATION

The Thin-ply "Advantage": new material

2018, $[45^\circ, 90^\circ, -45^\circ, 0^\circ]_{nS}$

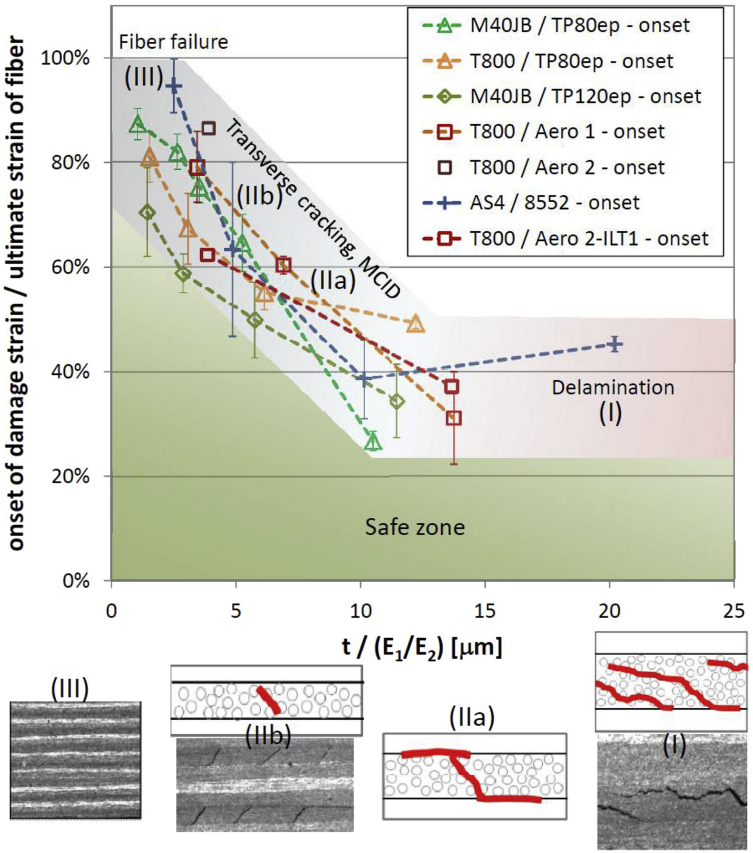

Cugnoni et al., Compos. Sci. Technol. **168**, 2018.

The Thin-ply "Advantage": new material, old result

2018, $[45^\circ, 90^\circ, -45^\circ, 0^\circ]_{nS}$

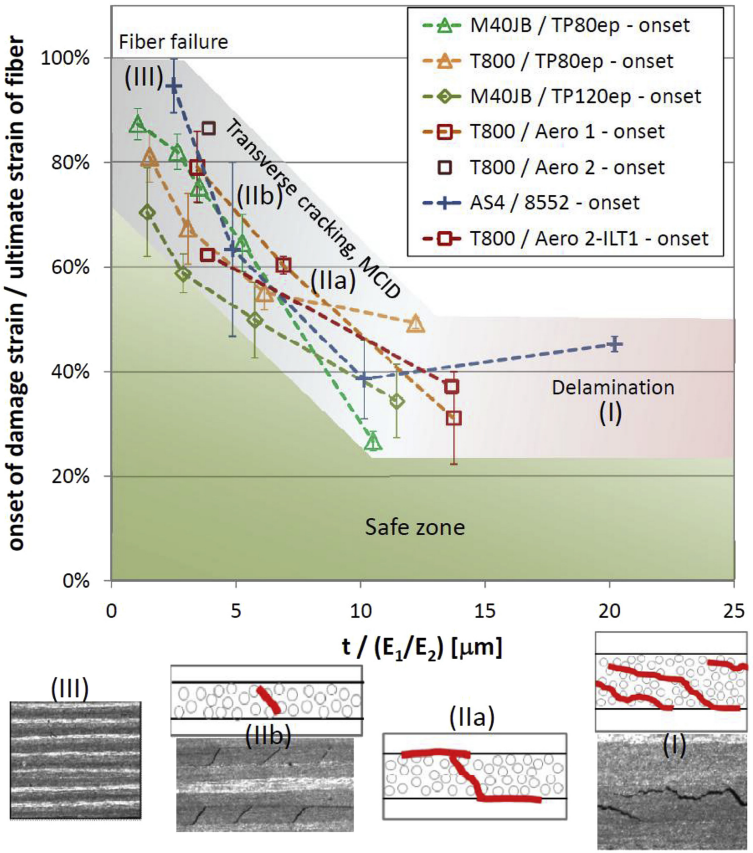

Cugnoni et al., Compos. Sci. Technol. **168**, 2018.

1979, $[0^\circ, 90^\circ_n]_S$

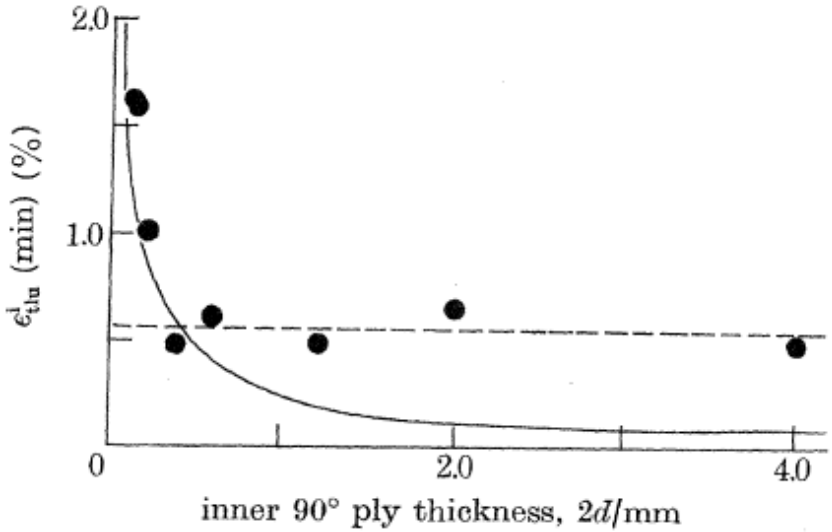

Bailey et al., P. Roy. Soc. A-Math. Phy. **366** (1727), 1979.

The Thin-ply "Advantage": new material, old result?

2018, $[45^\circ, 90^\circ, -45^\circ, 0^\circ]_{nS}$

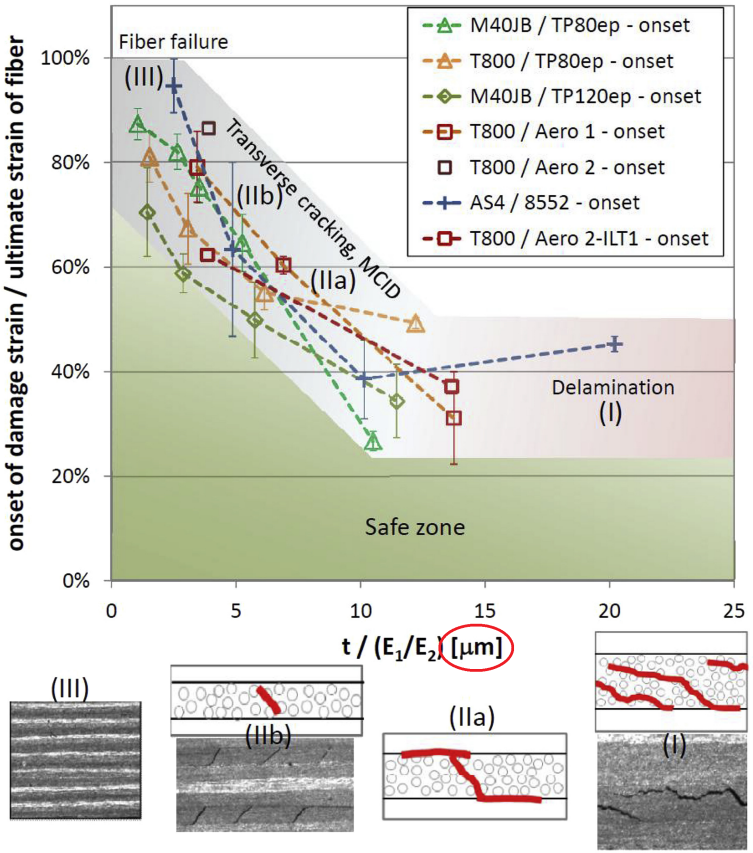

$t_{90^\circ} < 10 \varnothing_{fiber}$

Cugnoni et al., Compos. Sci. Technol. **168**, 2018.

1979, $[0^\circ, 90^\circ_n]_S$

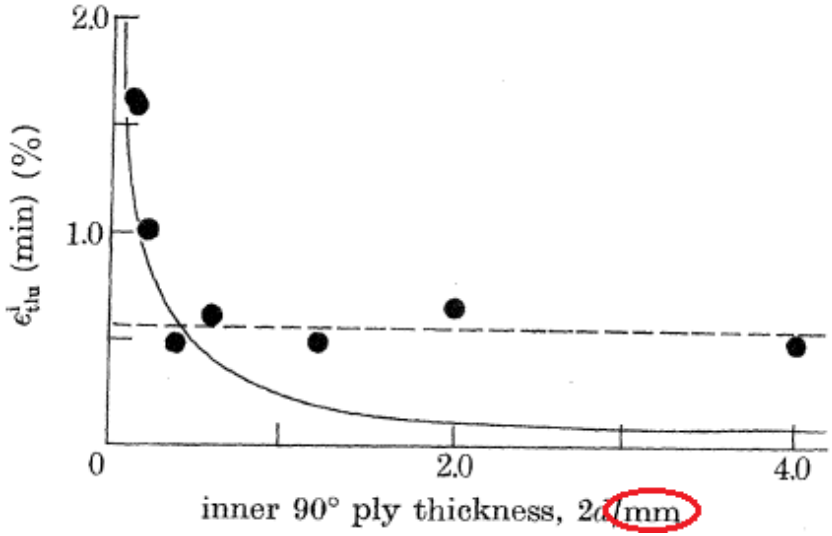

$t_{90^\circ} > 100 \varnothing_{fiber}$

Bailey et al., P. Roy. Soc. A-Math. Phy. **366** (1727), 1979.

Micromechanics of Initiation

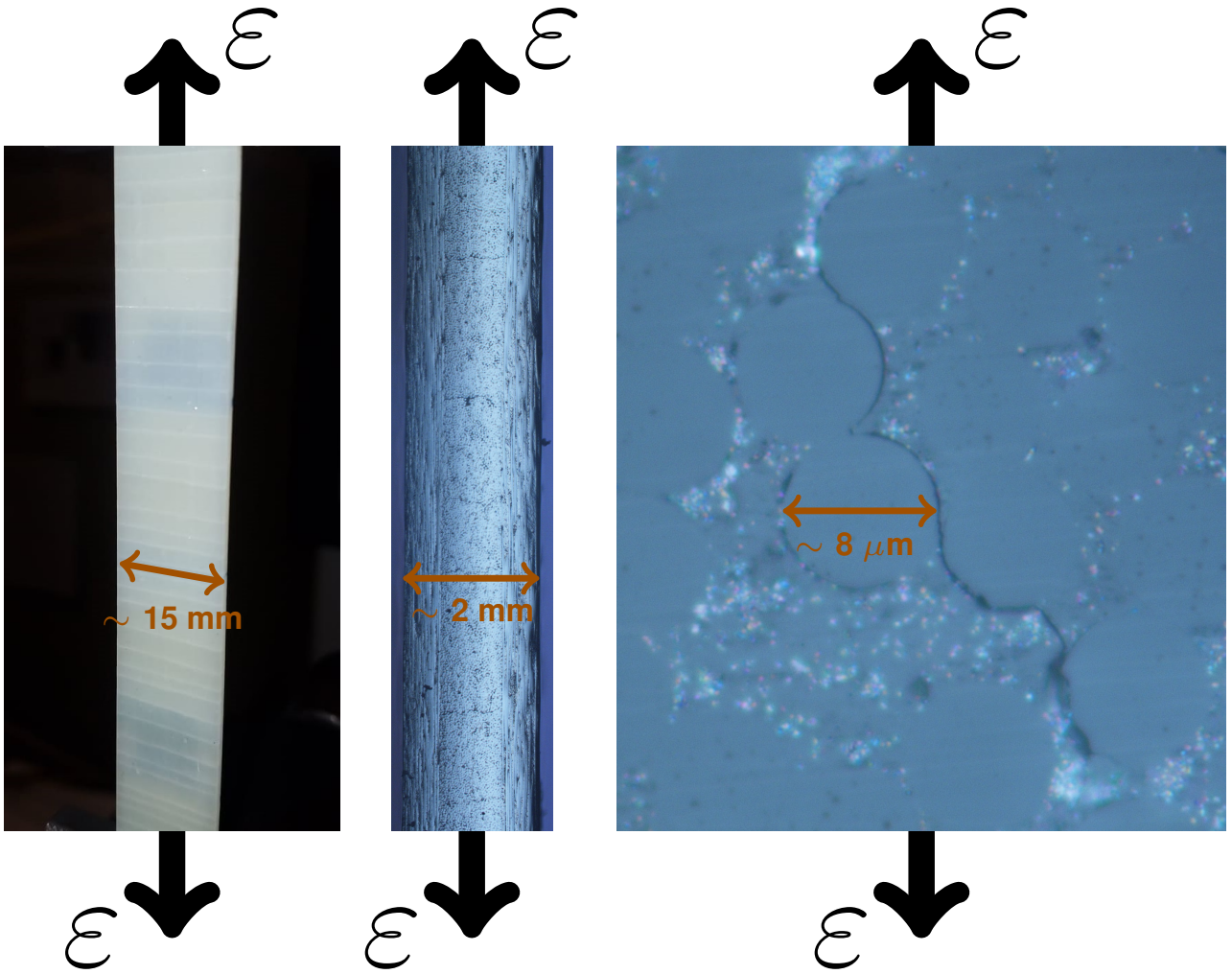

Left:
front view of $[0, 90_2]_S$, visual inspection.

Center:
edge view of $[0, 90]_S$, optical microscope.

Right:
edge view of $[0, 90]_S$, optical microscope.

Micromechanics of Initiation

Stage 1: isolated debonds

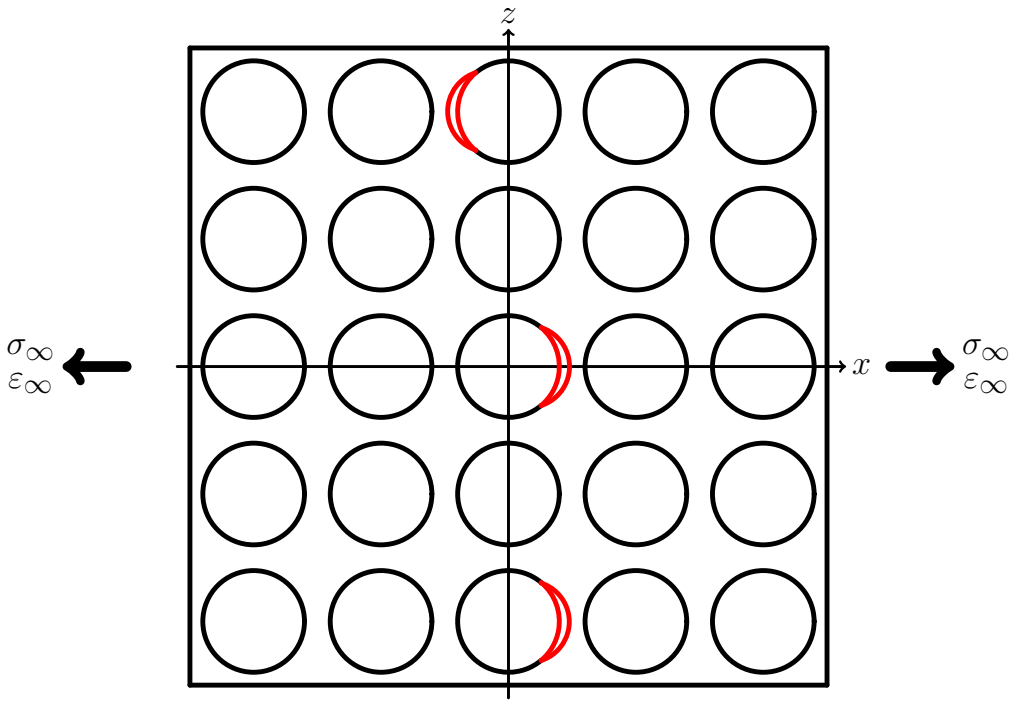

Bailey et al., P. Roy. Soc. A-Math. Phy. **366** (1727), 1979.

Bailey et al., J. Mater. Sci. **16** (3), 1981.

Zhang et al., Compos. Part A-Appl. S. **28** (4), 1997.

Micromechanics of Initiation

Stage 2: consecutive debonds

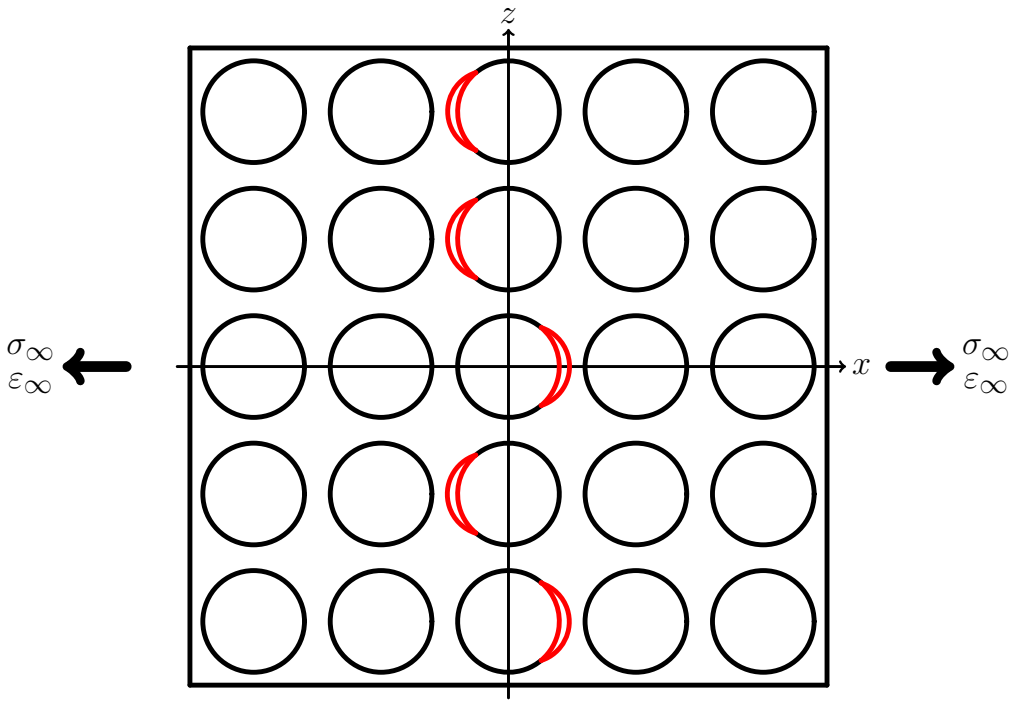

Bailey et al., P. Roy. Soc. A-Math. Phy. **366** (1727), 1979.

Bailey et al., J. Mater. Sci. **16** (3), 1981.

Zhang et al., Compos. Part A-Appl. S. **28** (4), 1997.

Micromechanics of Initiation

Stage 3: kinking

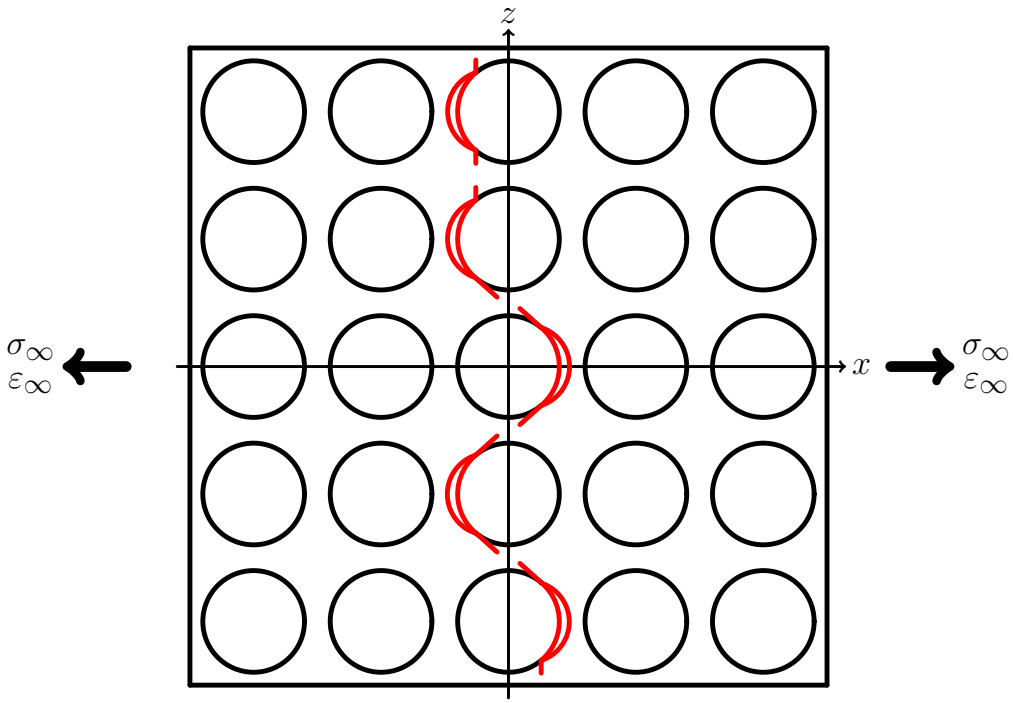

Bailey et al., P. Roy. Soc. A-Math. Phy. **366** (1727), 1979.

Bailey et al., J. Mater. Sci. **16** (3), 1981.

Zhang et al., Compos. Part A-Appl. S. **28** (4), 1997.

Micromechanics of Initiation

Stage 4: coalescence

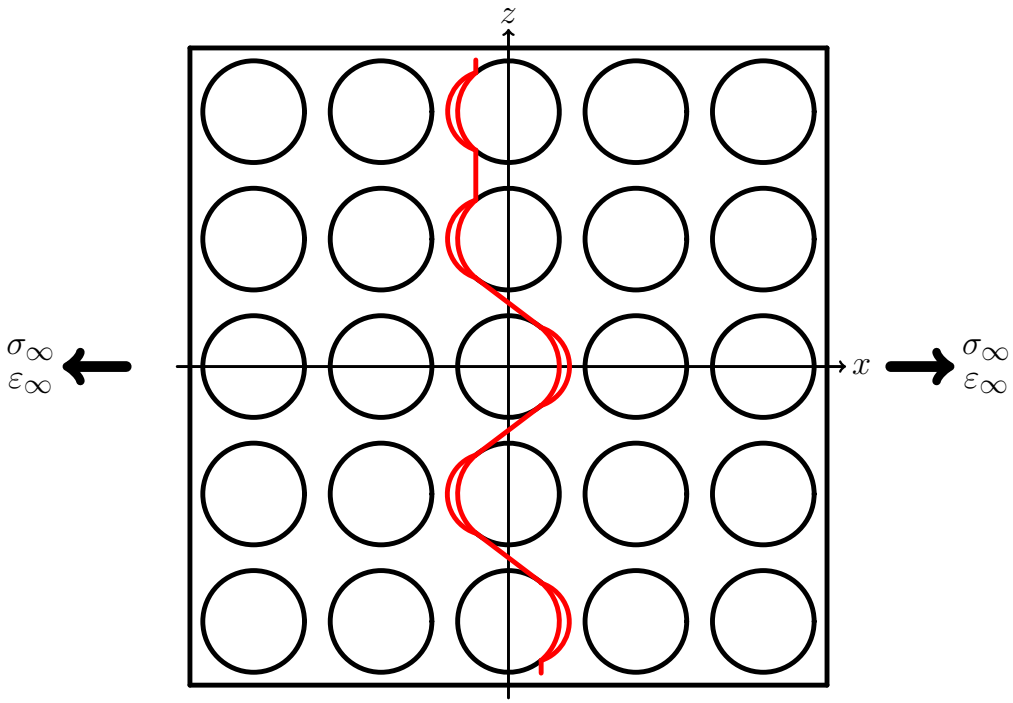

Bailey et al., P. Roy. Soc. A-Math. Phy. **366** (1727), 1979.

Bailey et al., J. Mater. Sci. **16** (3), 1981.

Zhang et al., Compos. Part A-Appl. S. **28** (4), 1997.

An Interesting Observation

$$[\mathbf{0}^\circ, \mathbf{90}^\circ_\mathbf{n}]_\mathbf{S}$$

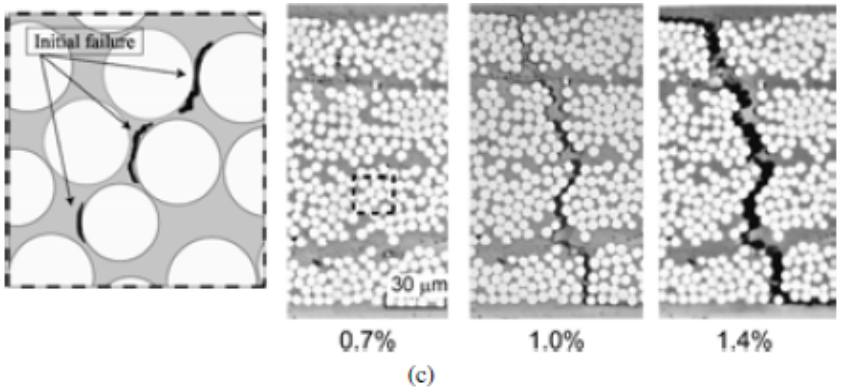

$n = 4$, $t_{90^\circ} = 160\mu m$

Saito et al., Adv. Compos. Mater. **21** (1), 2012.

An Interesting Observation

$$[\mathbf{0}^\circ, \mathbf{90}^\circ_\mathbf{n}]_\mathbf{S}$$

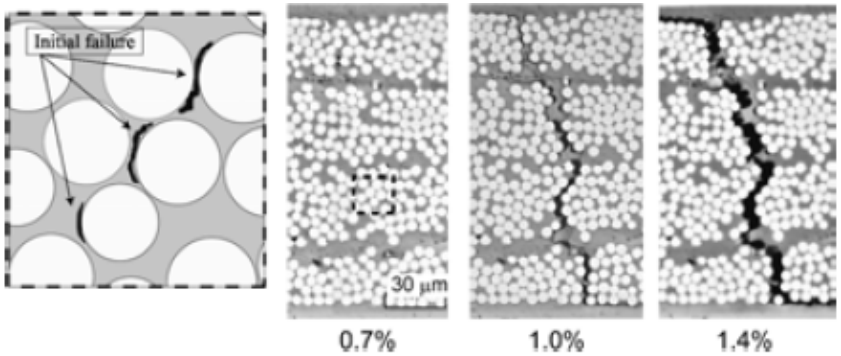

$n = 4$, $t_{90^\circ} = 160\mu m$

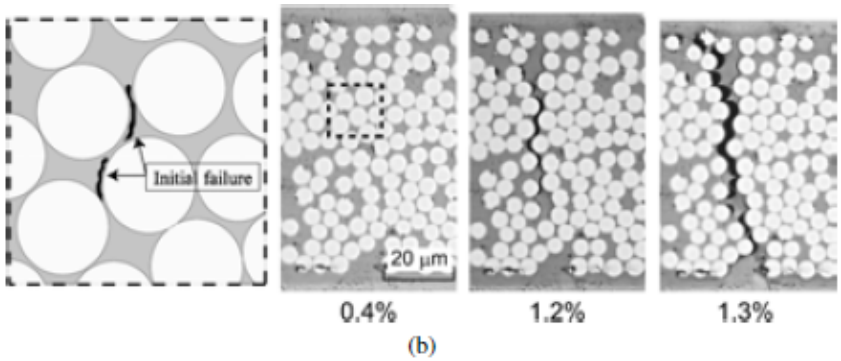

$n = 2$, $t_{90^\circ} = 80\mu m$

Saito et al., Adv. Compos. Mater. **21** (1), 2012.

An Interesting Observation

$$[\mathbf{0}^\circ, \mathbf{90}^\circ_\mathbf{n}]_\mathbf{S}$$

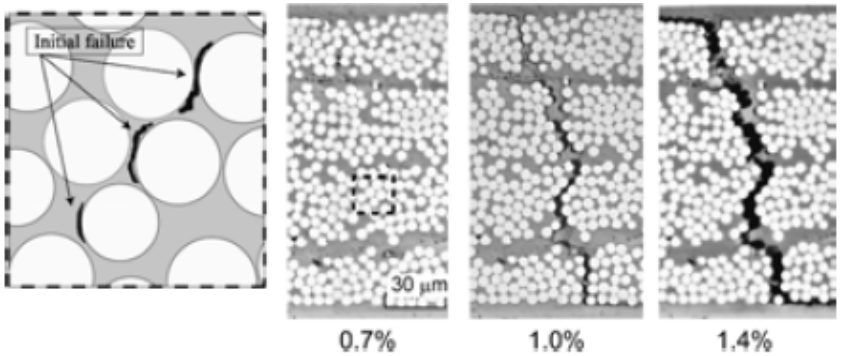

$n = 4$, $t_{90^\circ} = 160\mu m$

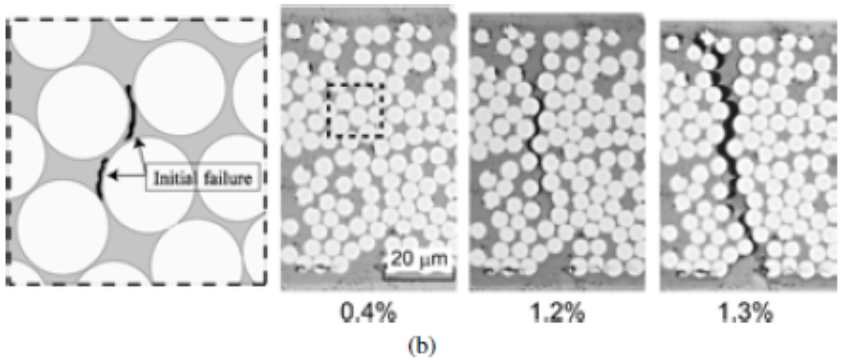

$n = 2$, $t_{90^\circ} = 80\mu m$

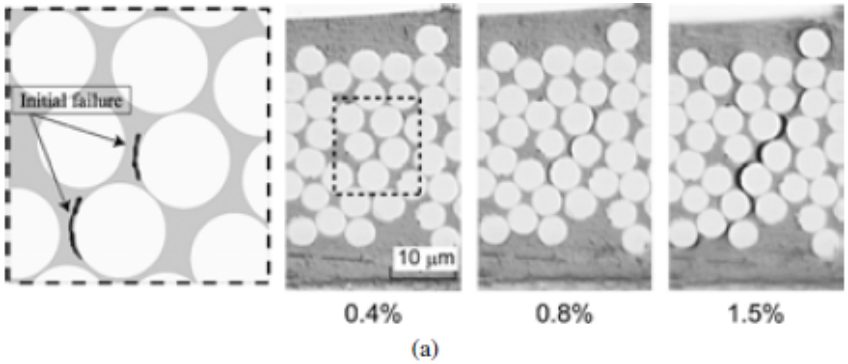

$n = 1$, $t_{90^\circ} = 40\mu m$

Saito et al., Adv. Compos. Mater. **21** (1), 2012.

Objectives

90° layer thickness and 0° layer thickness: what are their their effects on fiber-matrix interface crack growth?

Stage 1: isolated debonds

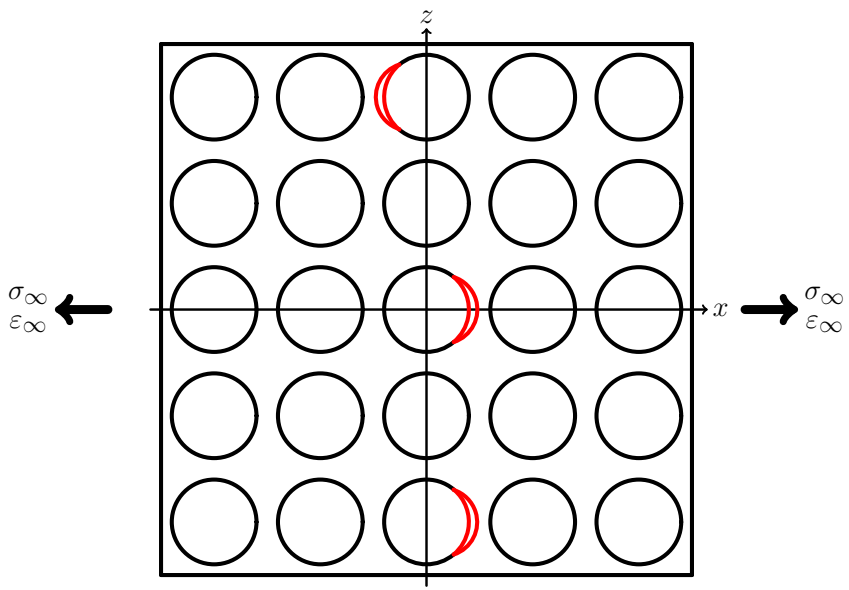

↘ MODELING

Geometry

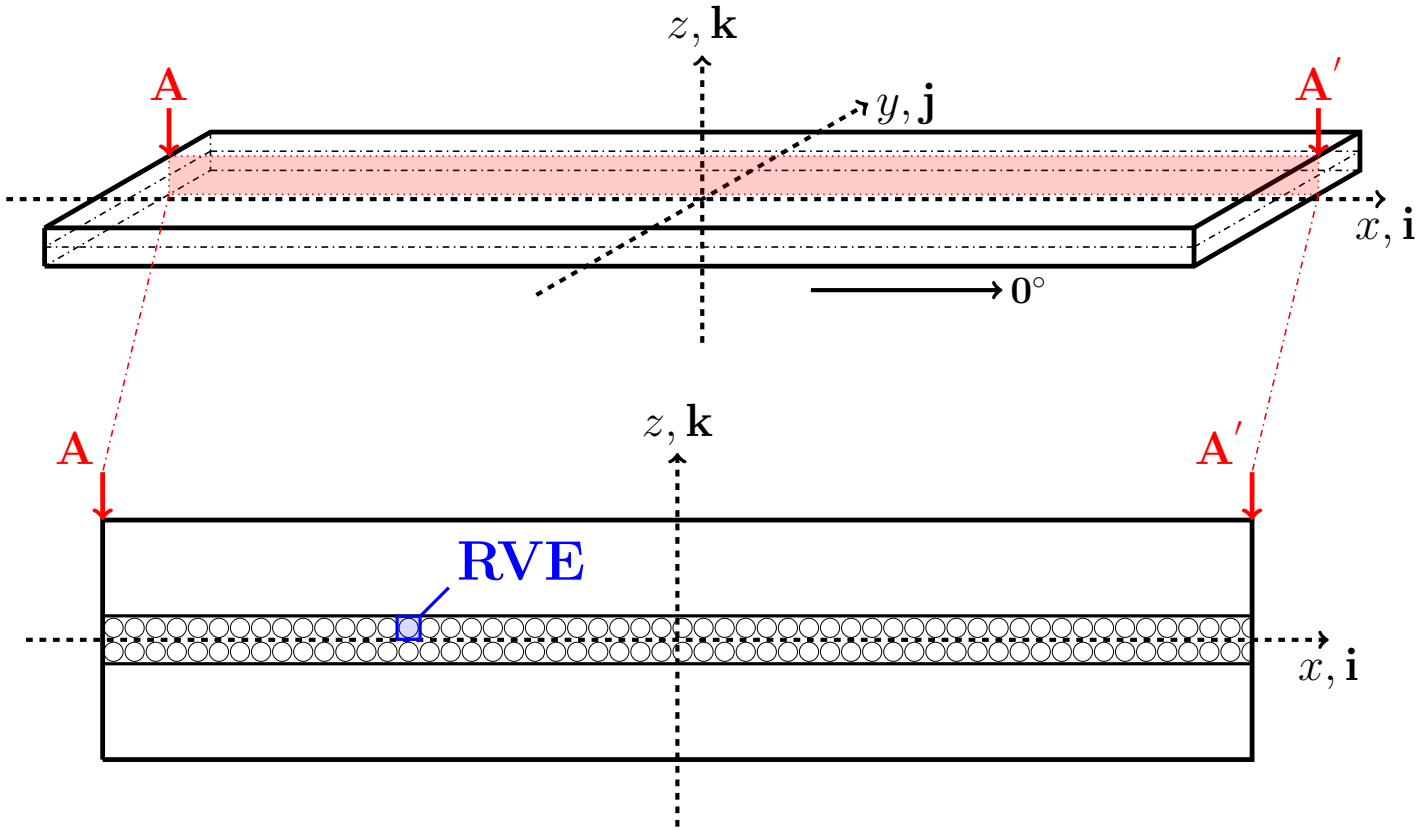

- ➔ $L, W >> t$
- ➔ $L, W \to \infty$
- ➔ Square packing
- ➔ $L_d >> \Delta\theta_d$
- ➔ 2D RVE

Representative Volume Elements

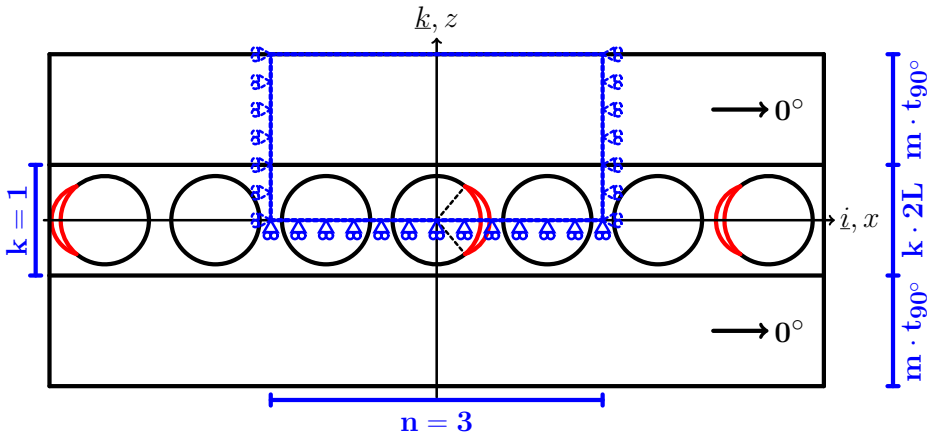

$$n \times 1 - m \cdot t_{90^\circ}$$

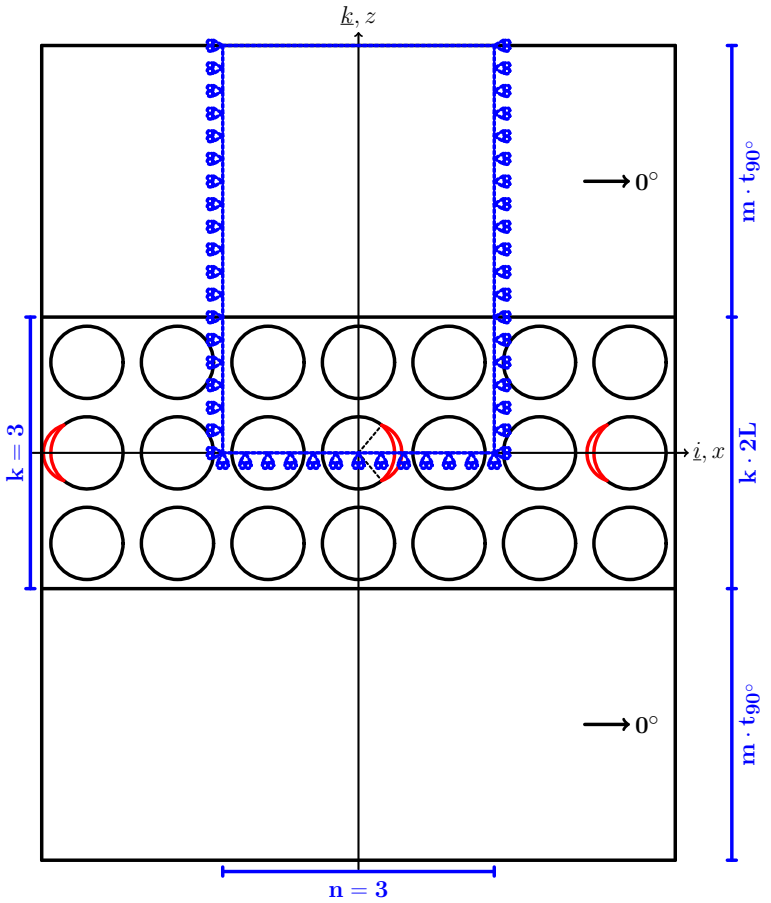

$$n \times k - m \cdot t_{90^\circ}$$

Representative Volume Elements

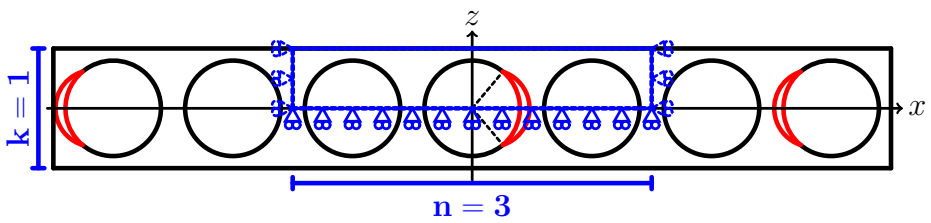

- *free*
- $n \times 1$ – *coupling*
- *coupling* + *H*

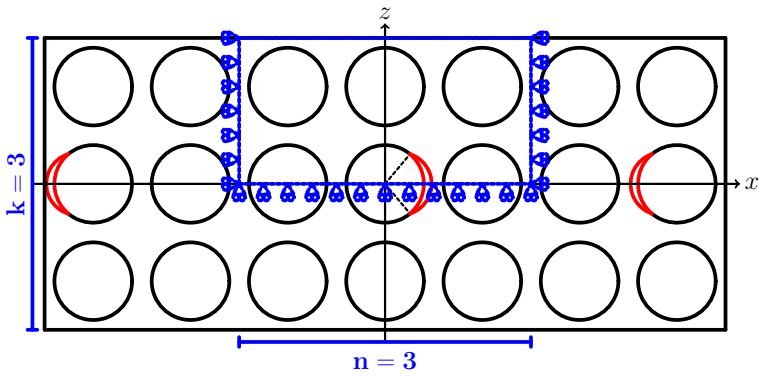

- *free*
- $n \times k$ – *coupling*
- *coupling* + *H*

Assumptions

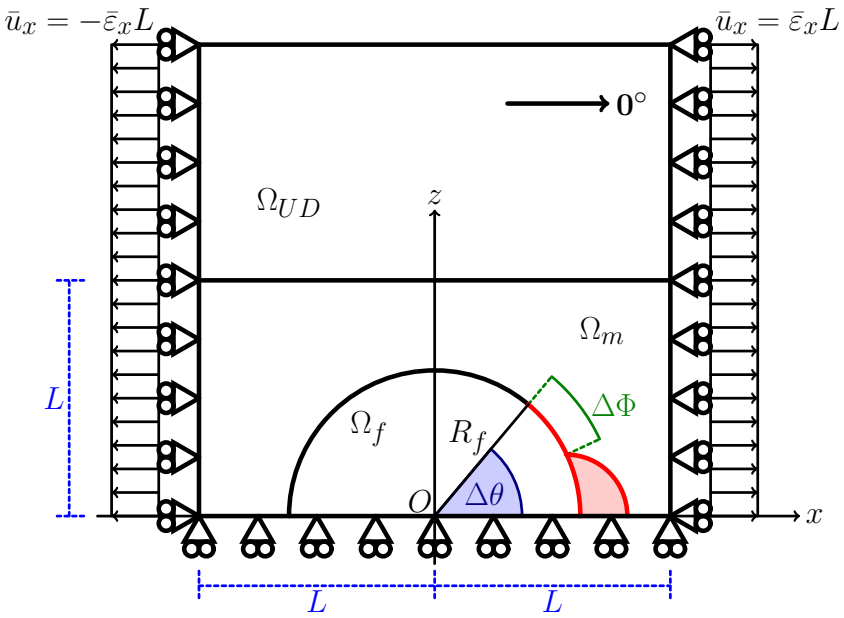

$$R_f = 1 \ [\mu m] \quad L = \frac{R_f}{2}\sqrt{\frac{\pi}{V_f}}$$

- ➔ Linear elastic, homogeneous materials
- ➔ Concentric Cylinders Assembly with Self-Consistent Shear Model for UD
- ➔ Plane strain
- ➔ Frictionless contact interaction
- ➔ Symmetric w.r.t. x-axis
- ➔ Coupling of x-displacements on left and right side (repeating unit cell)
- ➔ Applied uniaxial tensile strain $\bar{\varepsilon}_x = 1\%$
- ➔ $V_f = 60\%$

Material	V_f [%]	E_L [GPa]	E_T [GPa]	μ_{LT} [GPa]	ν_{LT} [−]	ν_{TT} [−]
Glass fiber	-	70.0	70.0	29.2	0.2	0.2
Epoxy	-	3.5	3.5	1.25	0.4	0.4
UD	60.0	43.442	13.714	4.315	0.273	0.465

Solution

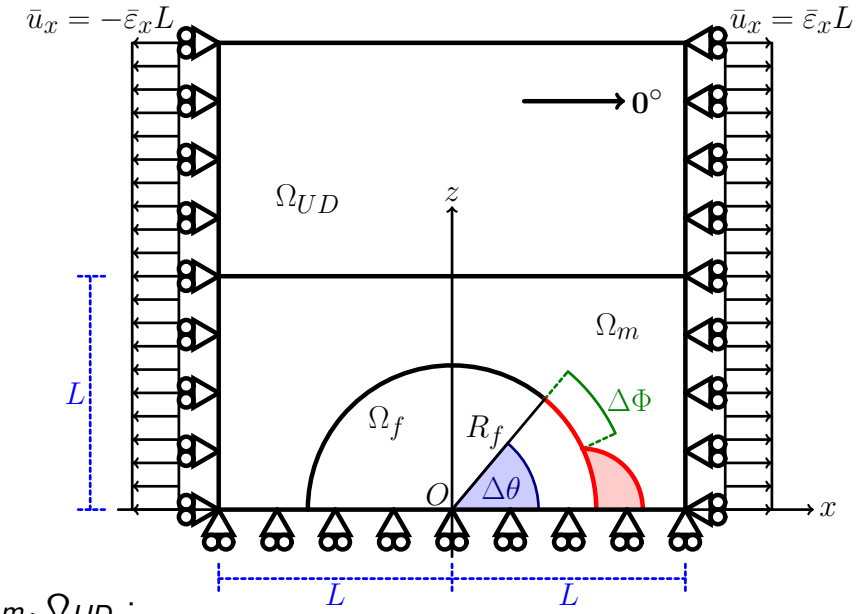

in $\Omega_f, \Omega_m, \Omega_{UD}$:

$$\frac{\partial^2 \varepsilon_{xx}}{\partial z^2} + \frac{\partial^2 \varepsilon_{zz}}{\partial x^2} = \frac{\partial^2 \gamma_{zx}}{\partial x \partial z}$$

$$\varepsilon_y = \gamma_{xy} = \gamma_{yz} = 0$$

$$\frac{\partial \sigma_{xx}}{\partial x} + \frac{\partial \tau_{zx}}{\partial z} = 0$$

$$\frac{\partial \tau_{zx}}{\partial x} + \frac{\partial \sigma_{zz}}{\partial z} = 0$$

$$\sigma_{yy} = \nu \left(\sigma_{xx} + \sigma_{zz} \right)$$

for $0^\circ \leq \alpha \leq \Delta\theta$:

$$\left(\vec{u}_m \left(R_f, \alpha \right) - \vec{u}_f \left(R_f, \alpha \right) \right) \cdot \vec{n}_\alpha \geq 0$$

for $\Delta\theta \leq \alpha \leq 180^\circ$:

$$\vec{u}_m \left(R_f, \alpha \right) - \vec{u}_f \left(R_f, \alpha \right) = 0$$

$$\sigma_{ij} = E_{ijkl} \varepsilon_{kl}$$

$+ BC$

$\forall\ \Delta\theta \neq 0^\circ$

➔ oscillating singularity

$$\sigma \sim r^{-\frac{1}{2}} \sin\left(\varepsilon \log r \right), \quad V_f \to 0$$

$$\varepsilon = \frac{1}{2\pi} \log\left(\frac{1-\beta}{1+\beta} \right)$$

$$\beta = \frac{\mu_2 \left(\kappa_1 - 1 \right) - \mu_1 \left(\kappa_2 - 1 \right)}{\mu_2 \left(\kappa_1 + 1 \right) + \mu_1 \left(\kappa_2 + 1 \right)}$$

➔ receding contact

➔ $\dfrac{G\left(R_{f,2}\right)}{G\left(R_{f,1}\right)} = \dfrac{R_{f,2}}{R_{f,1}}, \dfrac{G\left(\bar{\varepsilon}_{x,2}\right)}{G\left(\bar{\varepsilon}_{x,1}\right)} = \dfrac{\bar{\varepsilon}_{x,2}^2}{\bar{\varepsilon}_{x,1}^2}$

➔ FEM + LEFM (VCCT)

➔ regular mesh of quadrilaterals at the crack tip:

- $AR \sim 1, \quad \delta = 0.05^\circ$

$\forall\ \Delta\theta$

➔ 2^{nd} order shape functions

↘ Debond Initiation

σ_{rr} vs $\tau_{r\theta}$: radial stress vs tangential shear at the interface

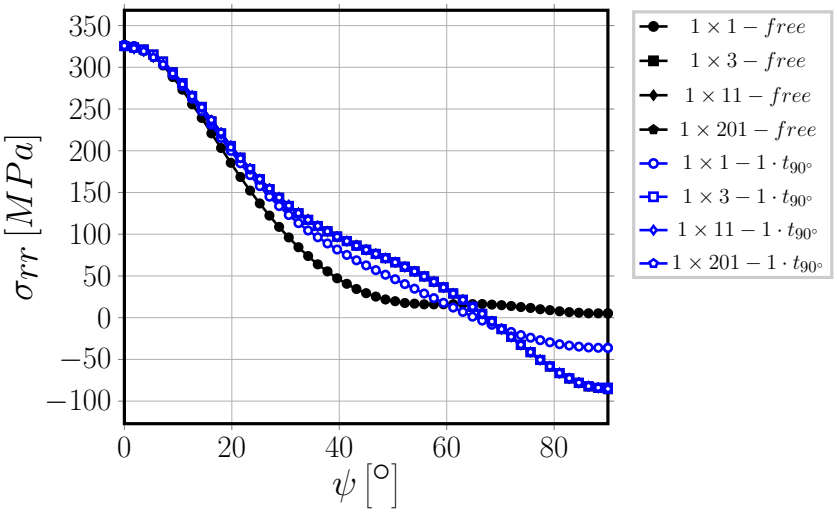

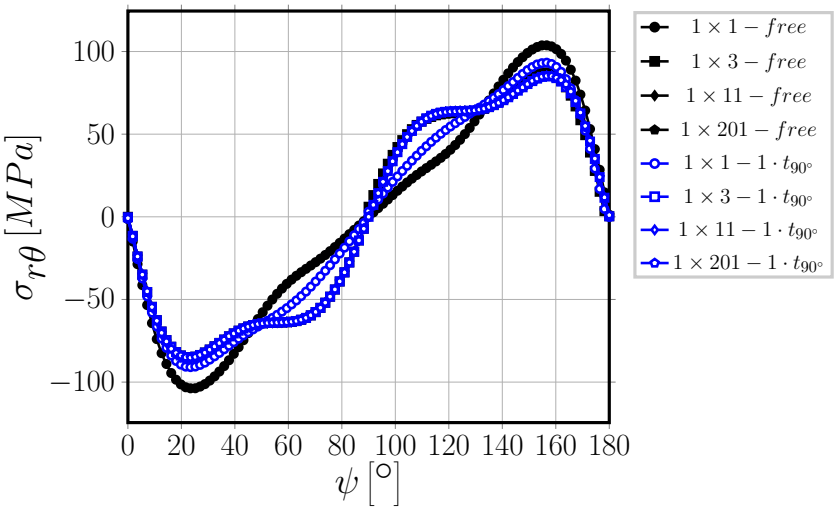

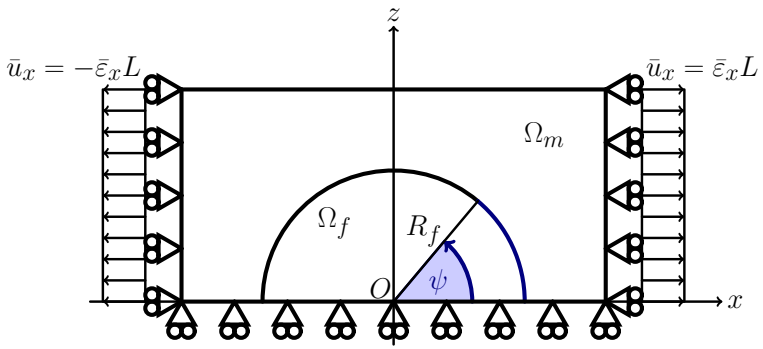

σ_{rr} vs $\tau_{r\theta}$: radial stress vs tangential shear at the interface

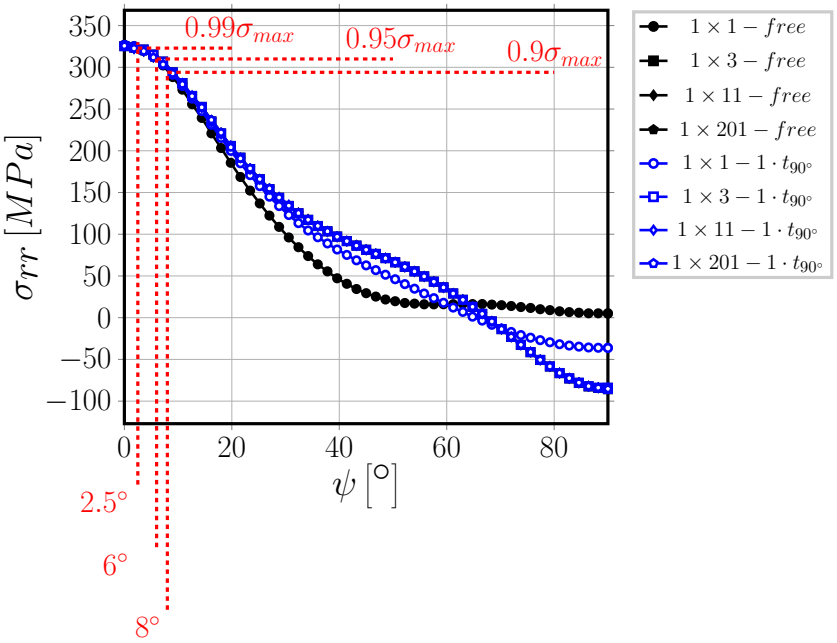

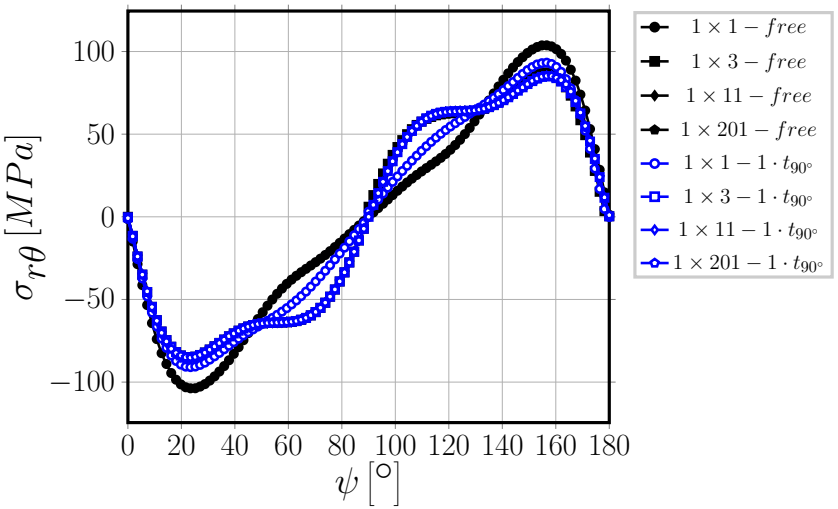

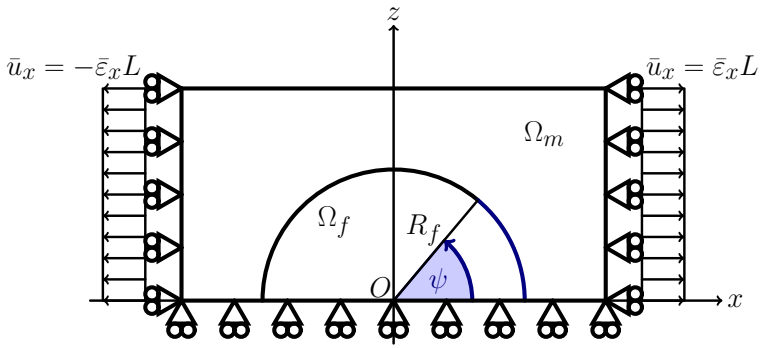

σ_{LHS}: local hydrostatic stress at the interface

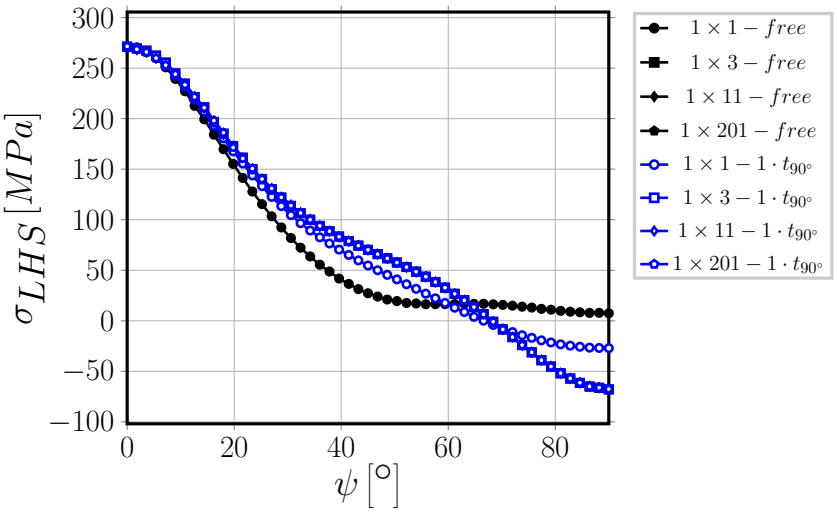

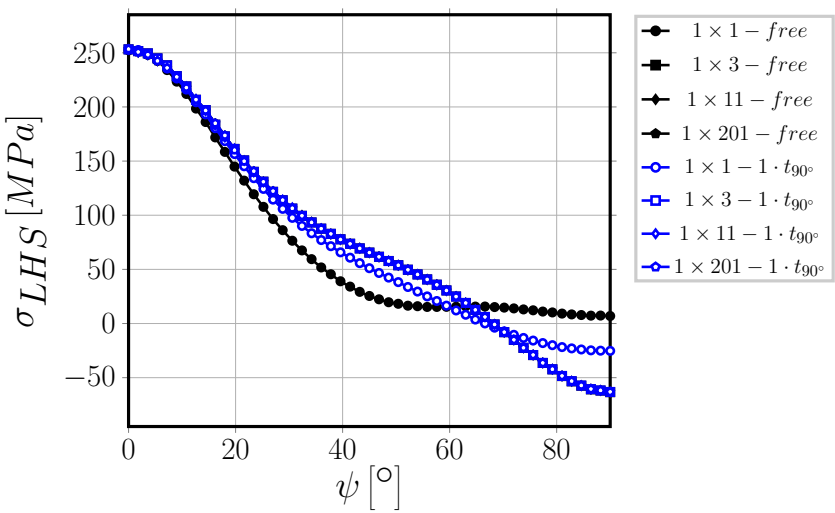

$$\sigma^{2D}_{LHS} = \frac{\sigma_{rr} + \sigma_{\theta\theta}}{2}$$

$$\sigma^{3D}_{LHS} = \frac{\sigma_{rr} + \sigma_{\theta\theta} + \sigma_{yy}}{3}$$

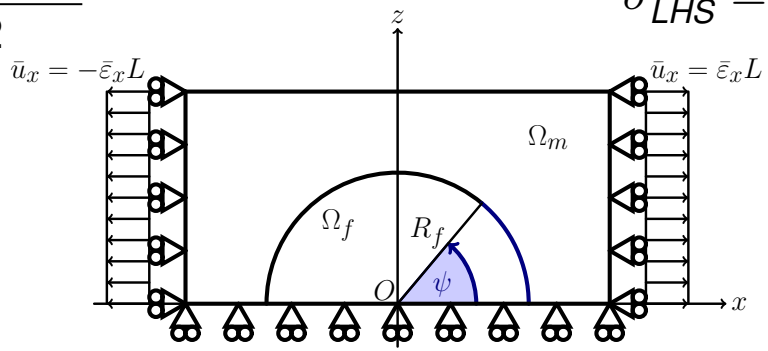

σ_{LHS}: local hydrostatic stress at the interface

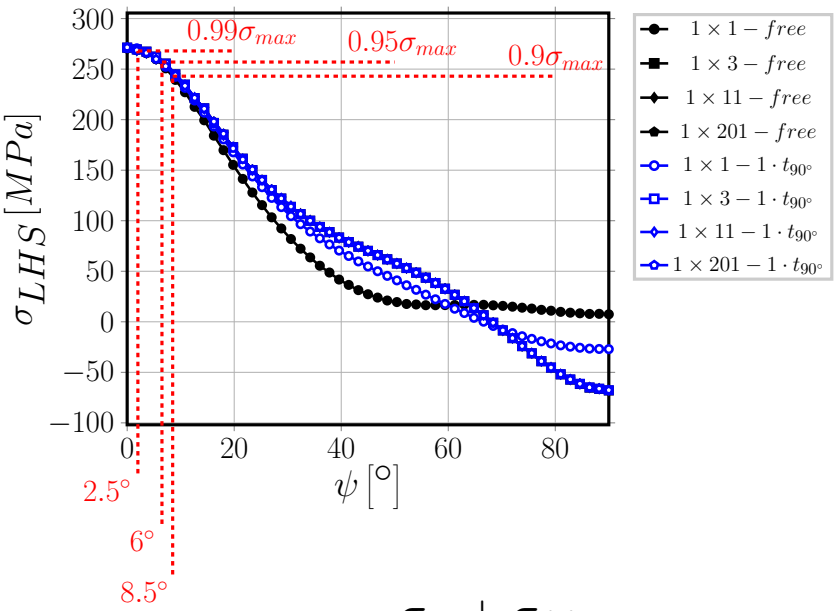

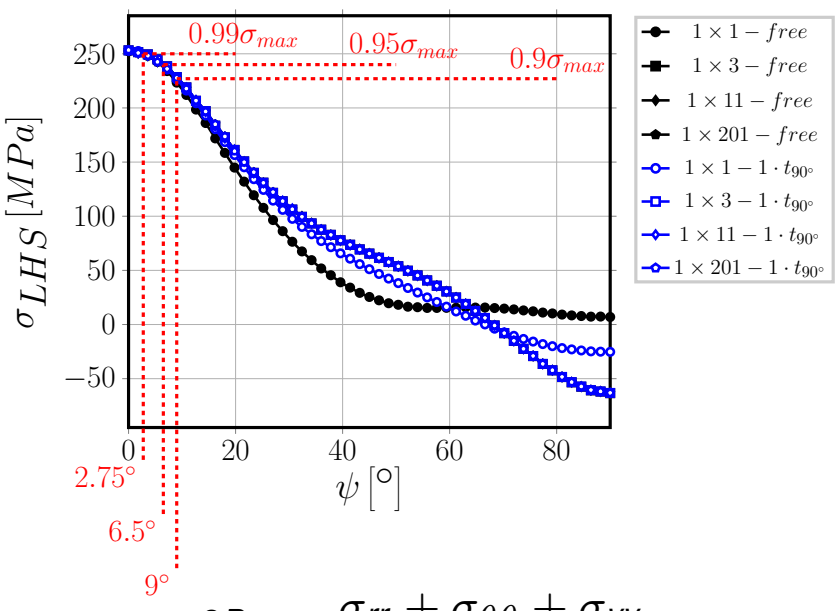

$$\sigma^{2D}_{LHS} = \frac{\sigma_{rr} + \sigma_{\theta\theta}}{2}$$

$$\sigma^{3D}_{LHS} = \frac{\sigma_{rr} + \sigma_{\theta\theta} + \sigma_{yy}}{3}$$

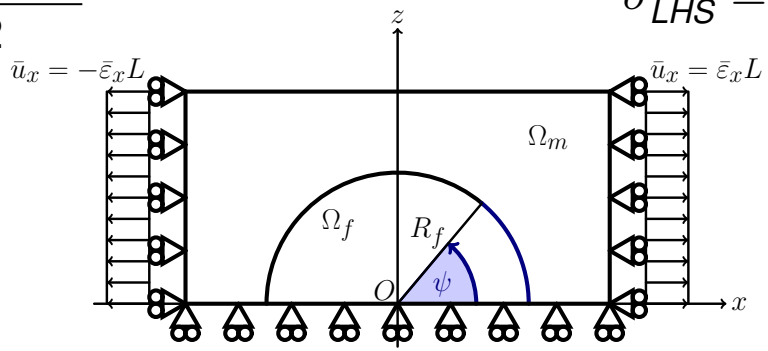

σ_{vM}: von Mises stress at the interface

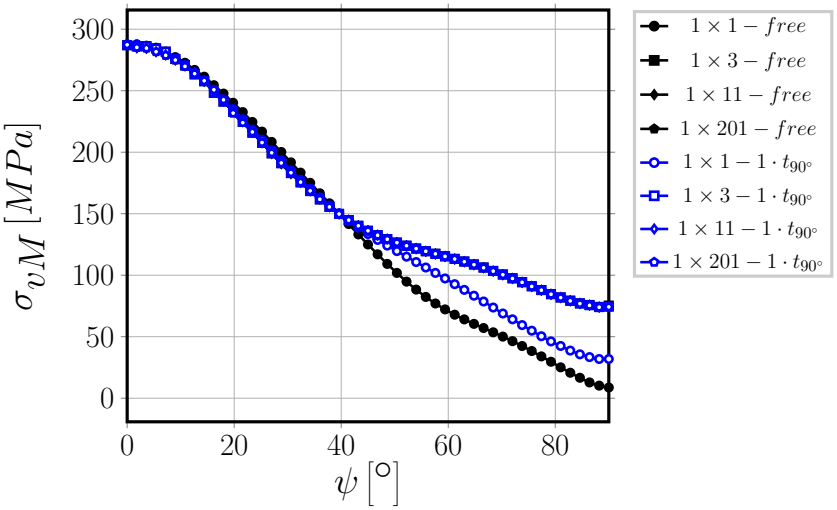

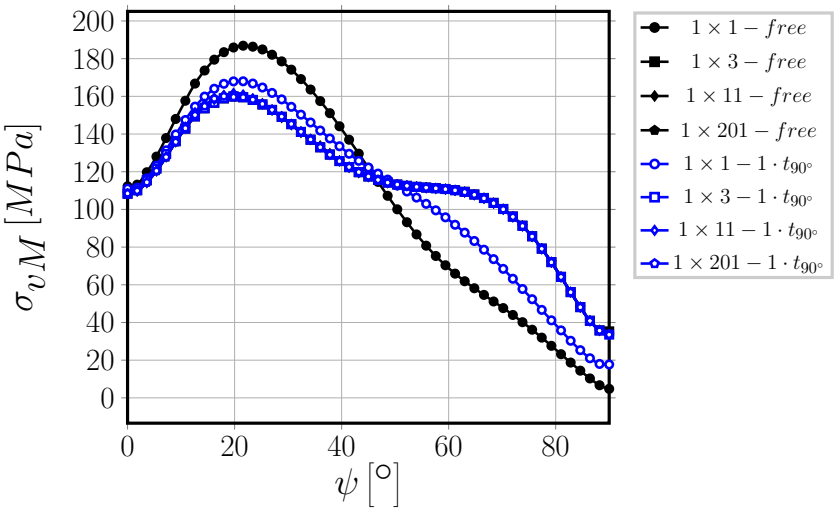

$$\sigma_{vM}^{2D} = \sqrt{(\sigma_{rr} - \sigma_{\theta\theta})^2 + 3\tau_{12}^2}$$

$$\sigma_{LHS}^{3D} = \frac{3}{2} s_{ij} s_{ij} \quad s_{ij} = \sigma_{ij} - \frac{1}{3}\sigma_{kk}\delta_{ij}$$

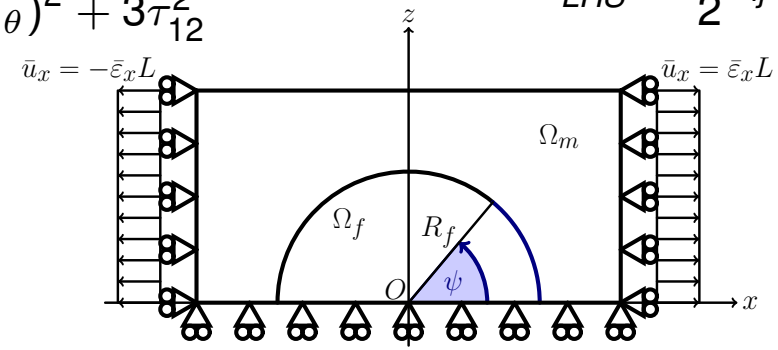

σ_{vM}: von Mises stress at the interface

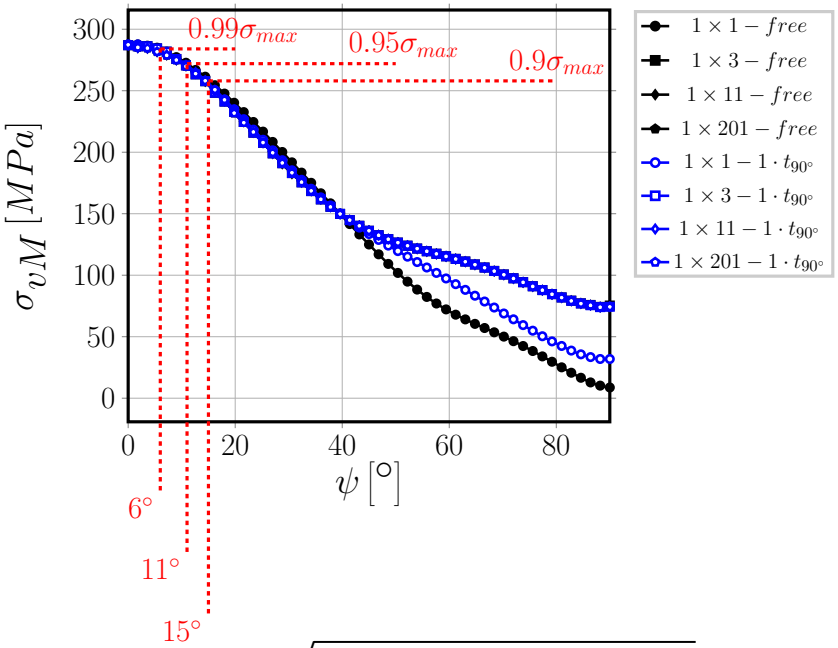

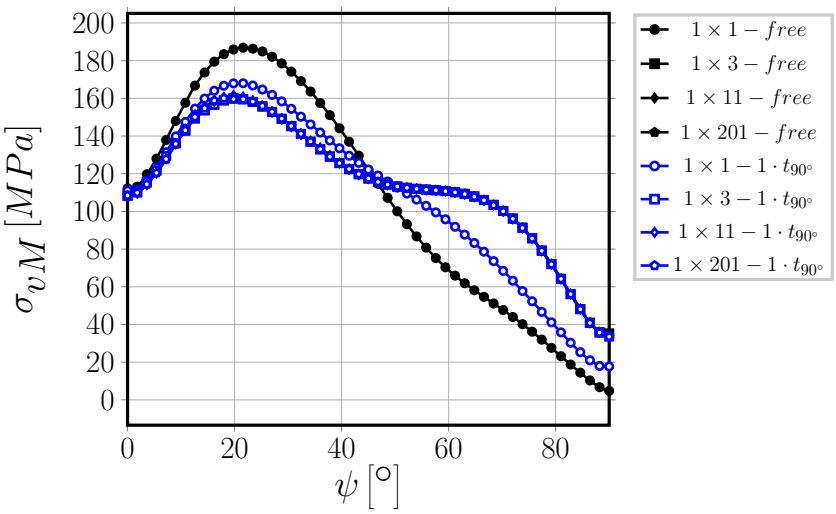

$$\sigma_{vM}^{2D} = \sqrt{(\sigma_{rr}-\sigma_{\theta\theta})^2 + 3\tau_{12}^2}$$

$$\sigma_{LHS}^{3D} = \frac{3}{2} s_{ij} s_{ij} \quad s_{ij} = \sigma_{ij} - \frac{1}{3}\sigma_{kk}\delta_{ij}$$

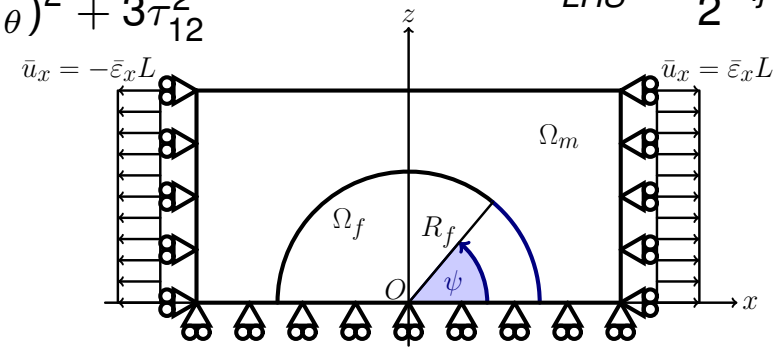

σ_I: maximum principal stress at the interface

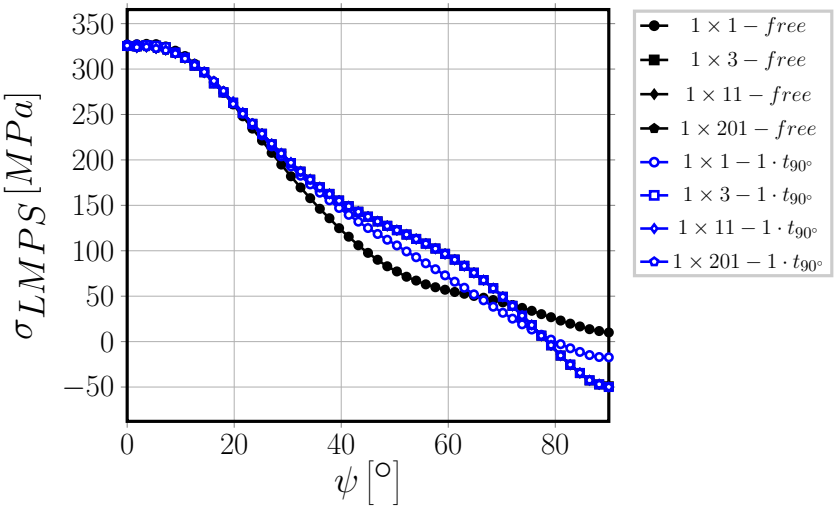

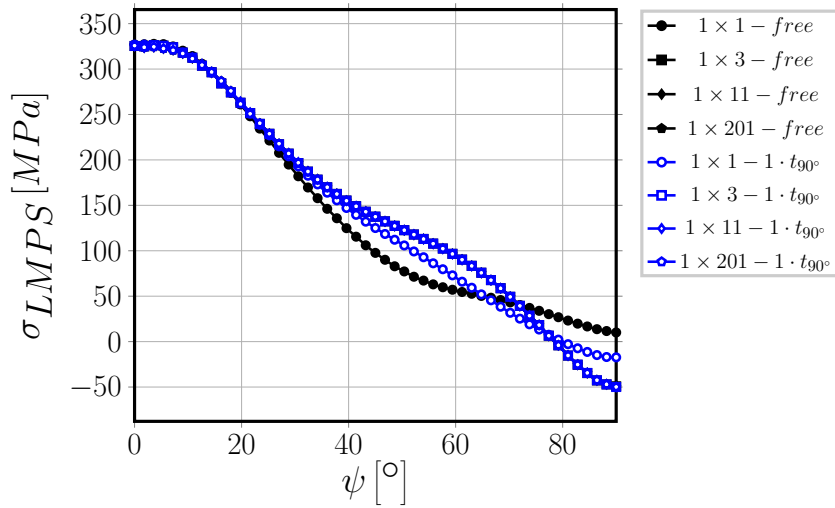

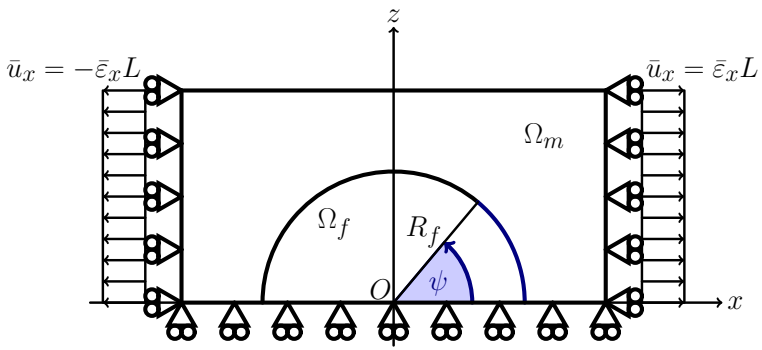

σ_I: maximum principal stress at the interface

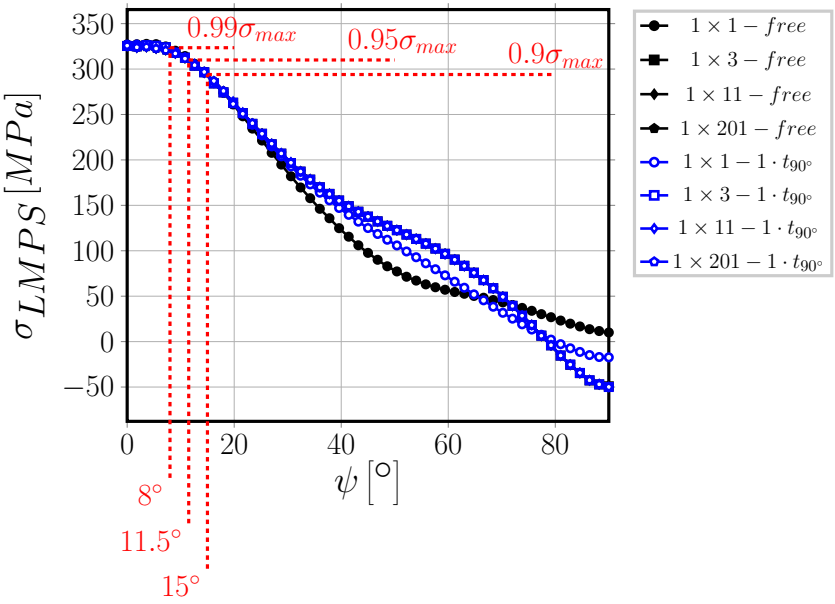

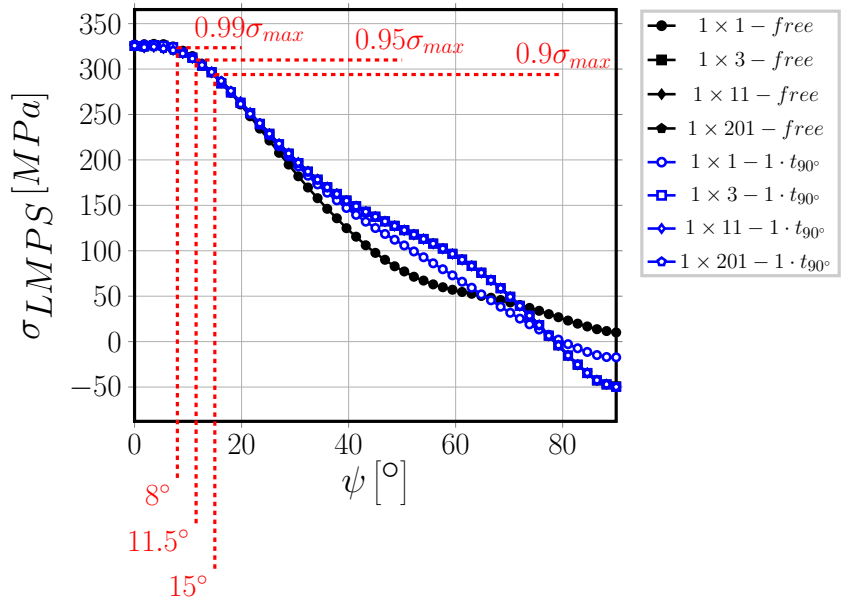

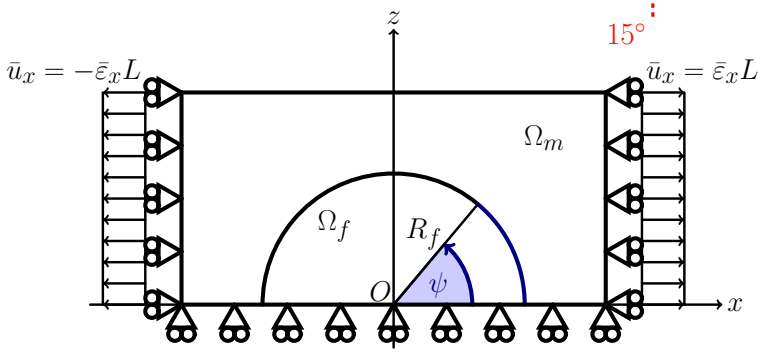

↘ Debond Propagation

Interaction of Debonds: Strain Magnification

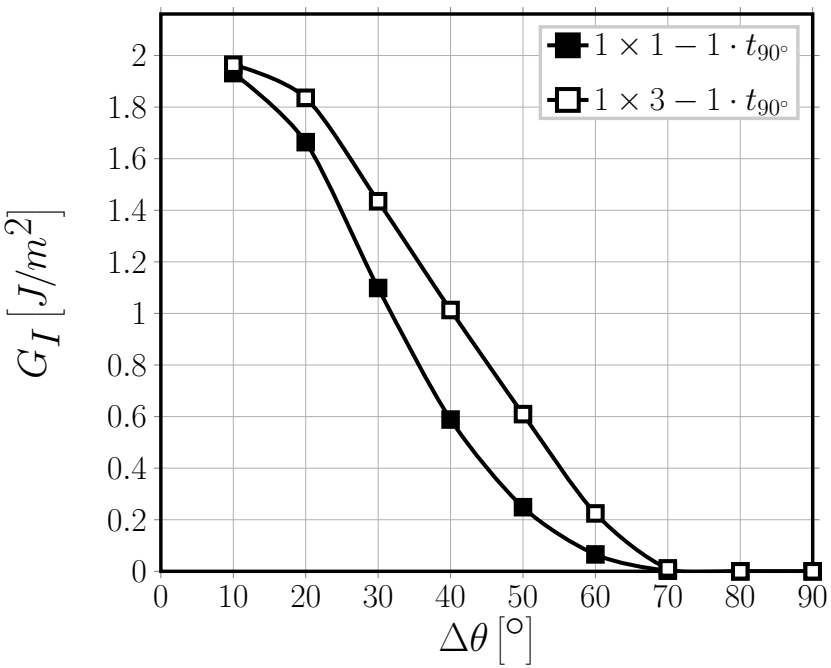

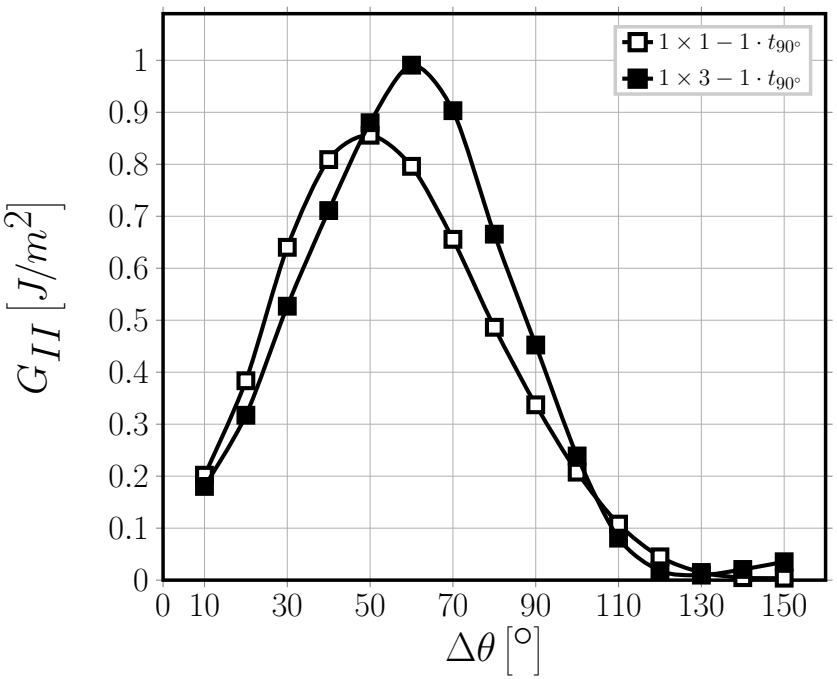

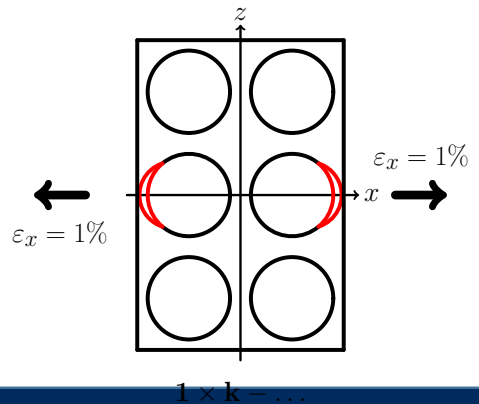

Interaction of Debonds: Strain Magnification

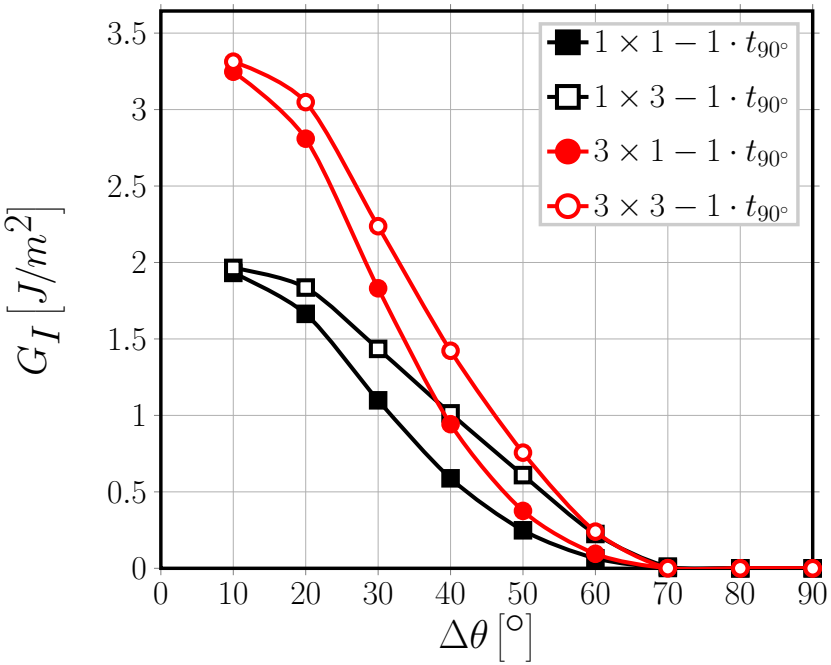

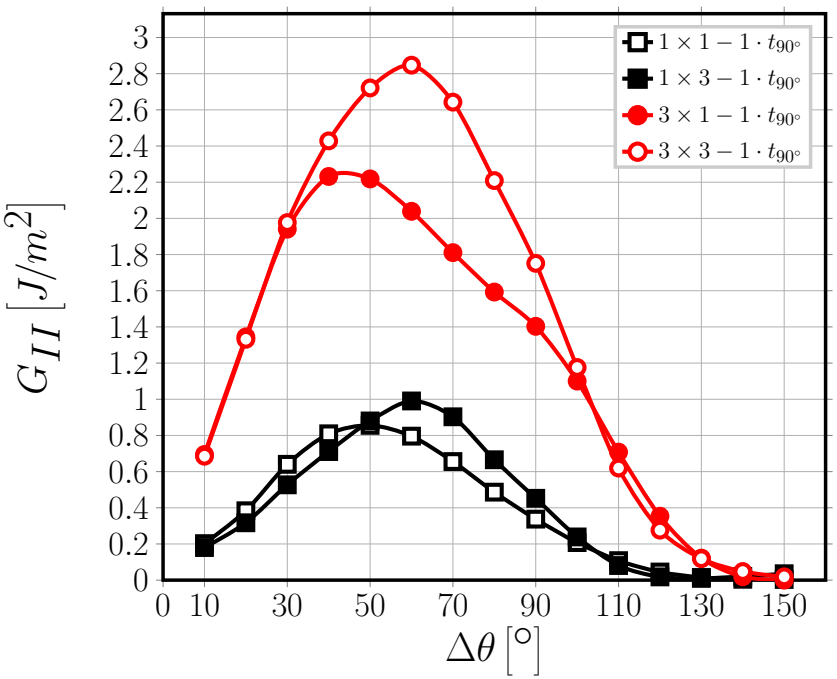

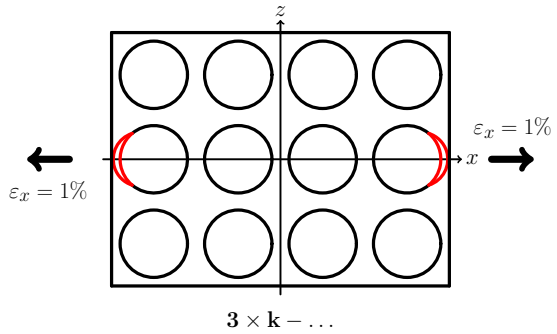

Interaction of Debonds: Strain Magnification

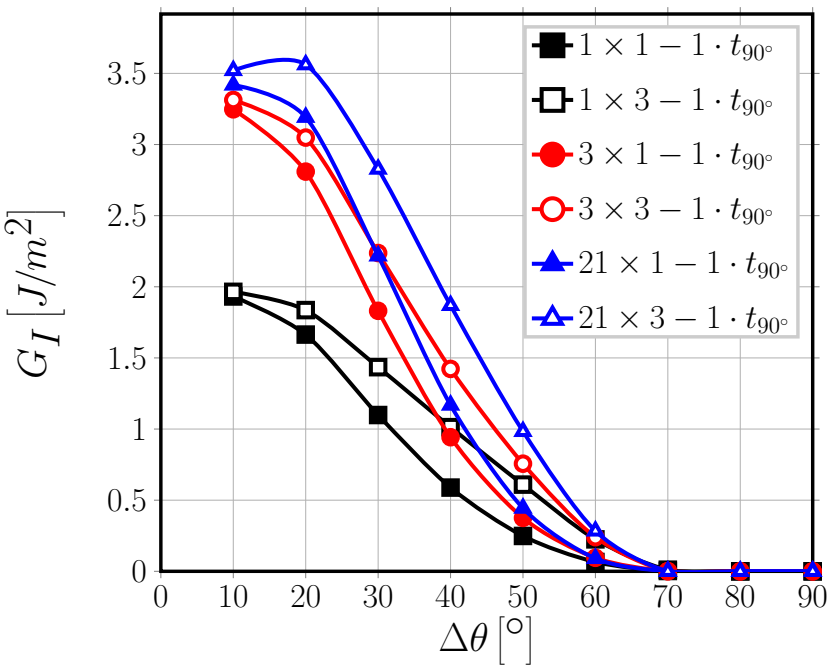

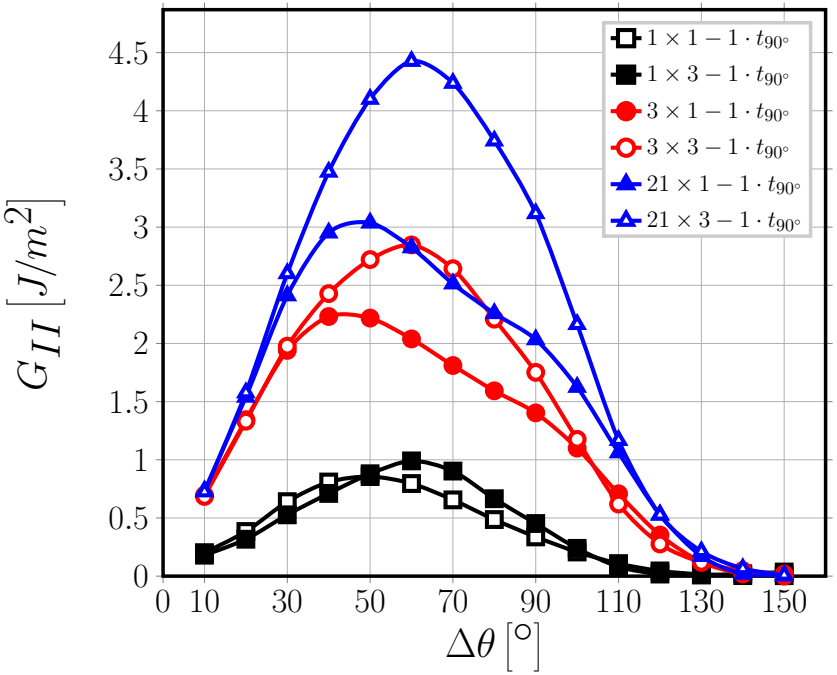

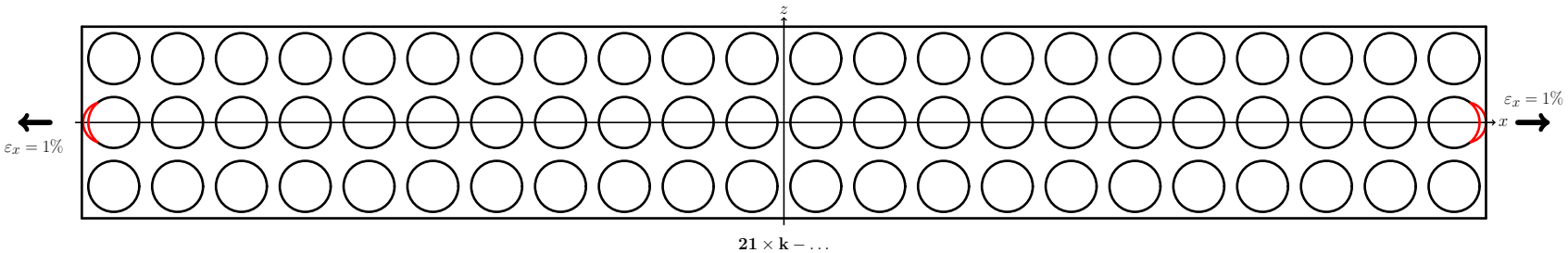

Interaction of Debonds: Crack Shielding

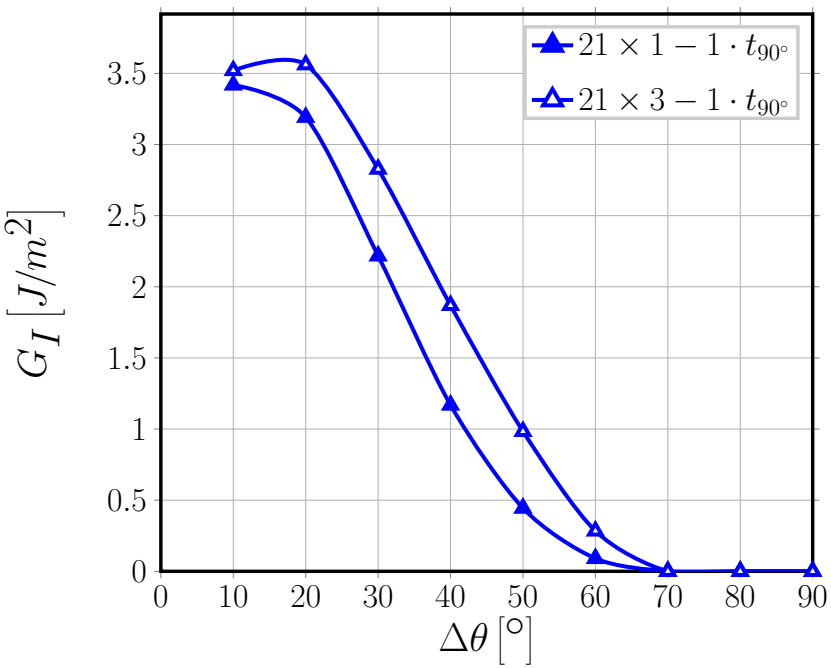

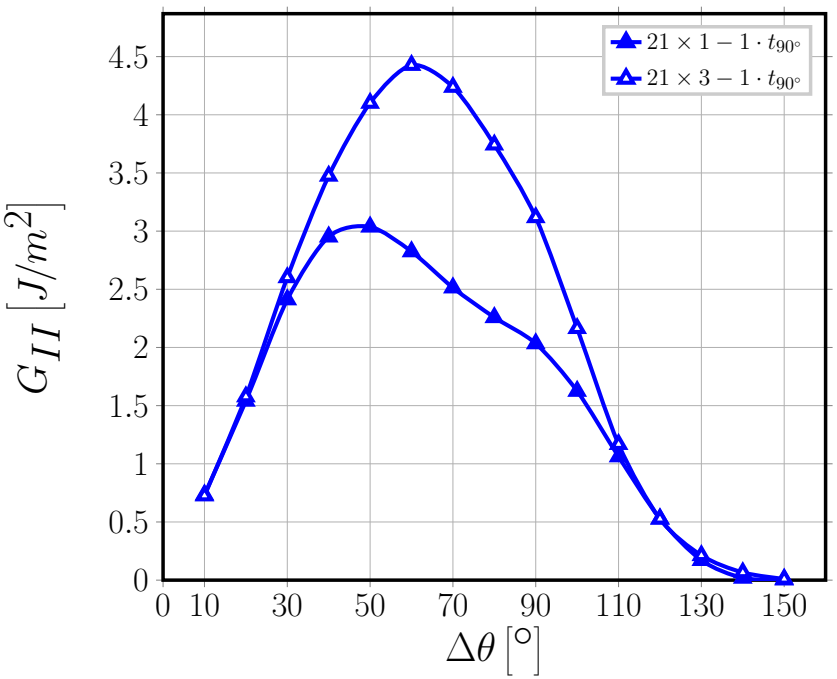

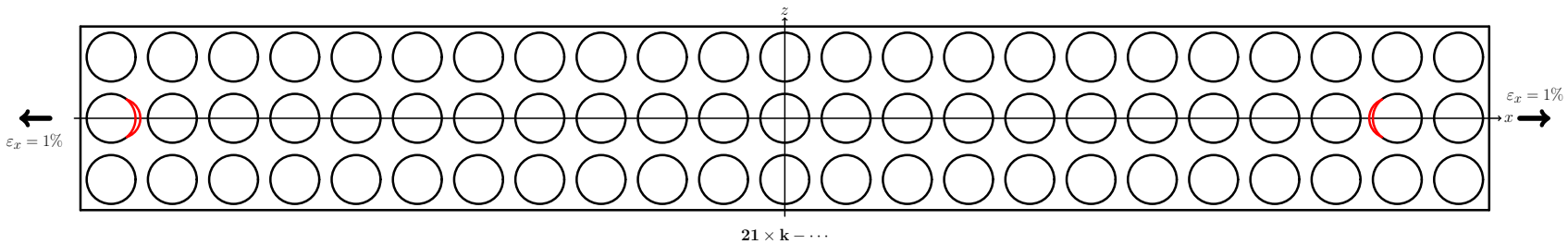

Interaction of Debonds: Crack Shielding

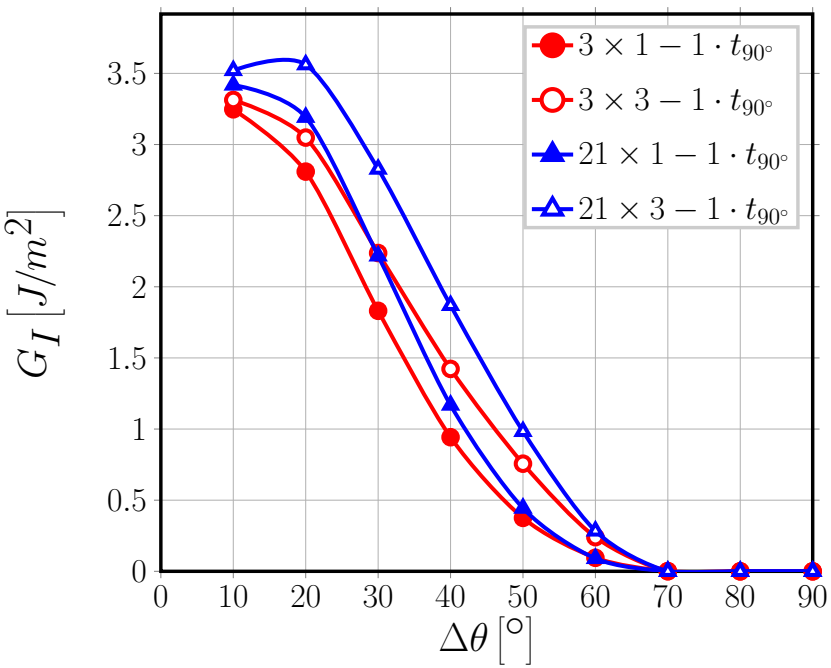

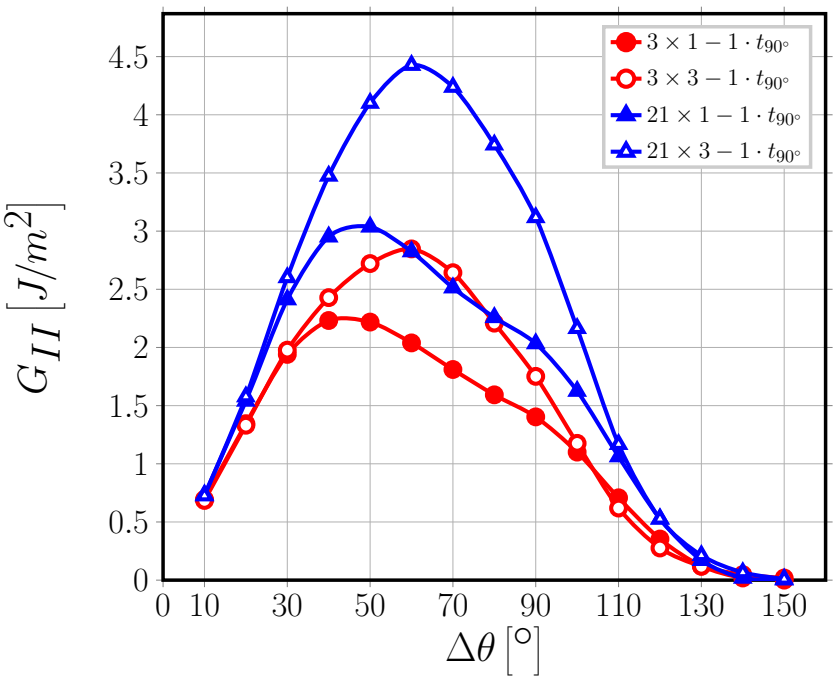

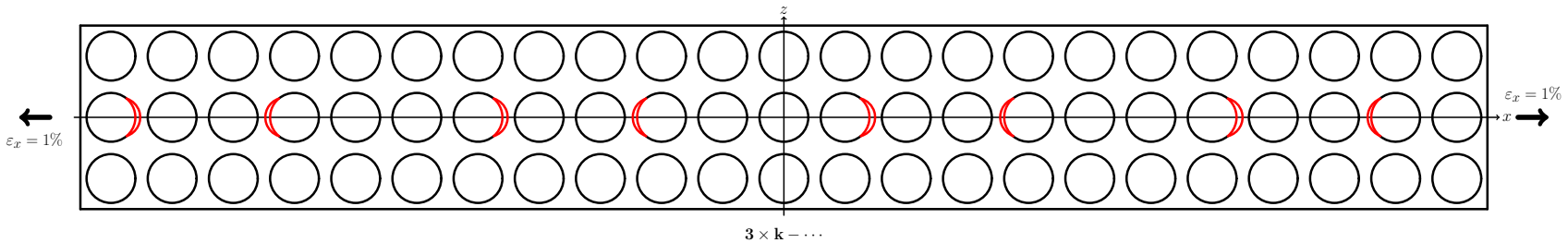

Interaction of Debonds: Crack Shielding

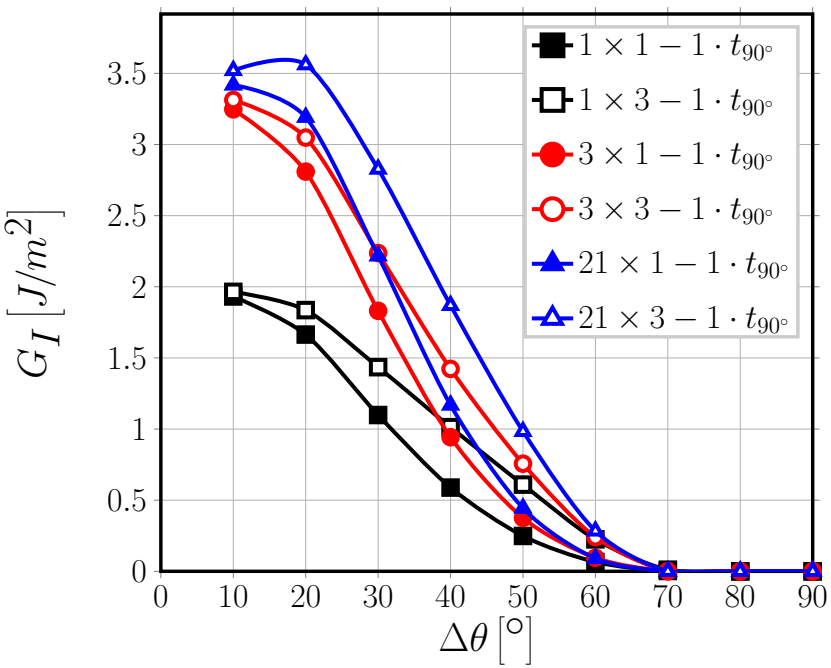

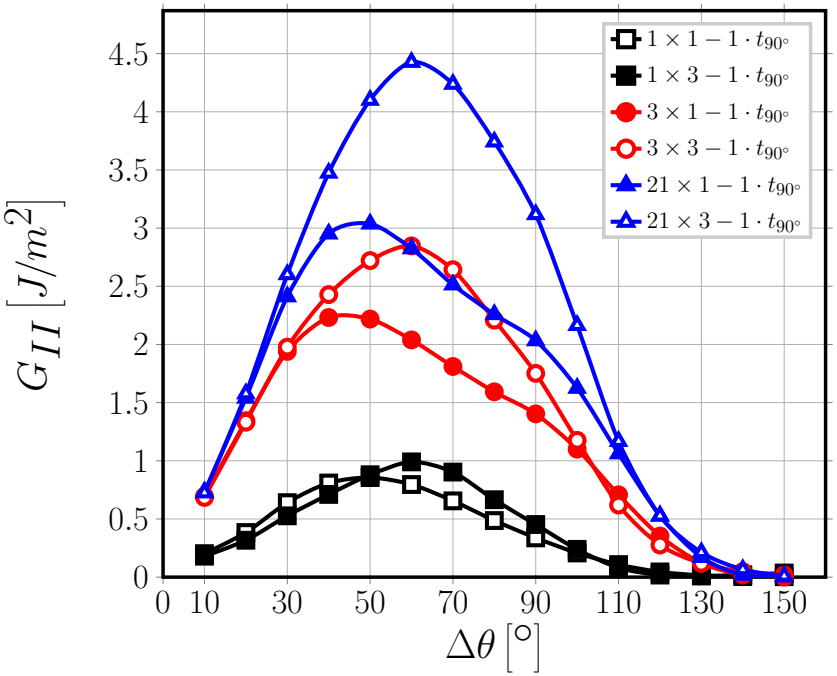

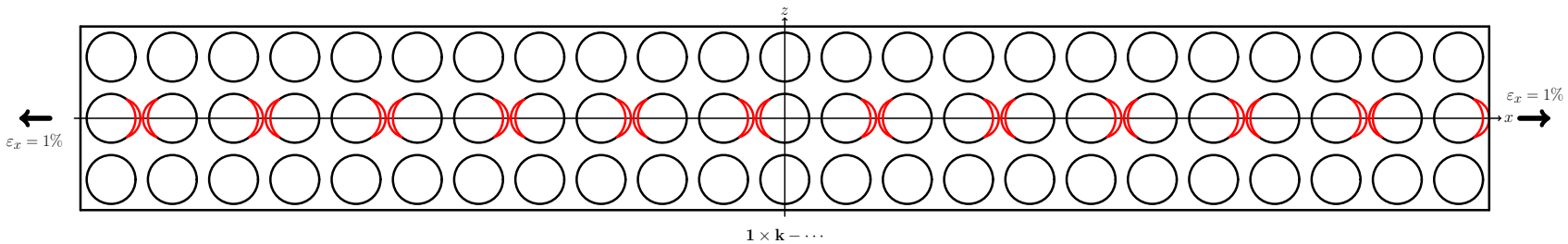

Effect of 0° ply thickness

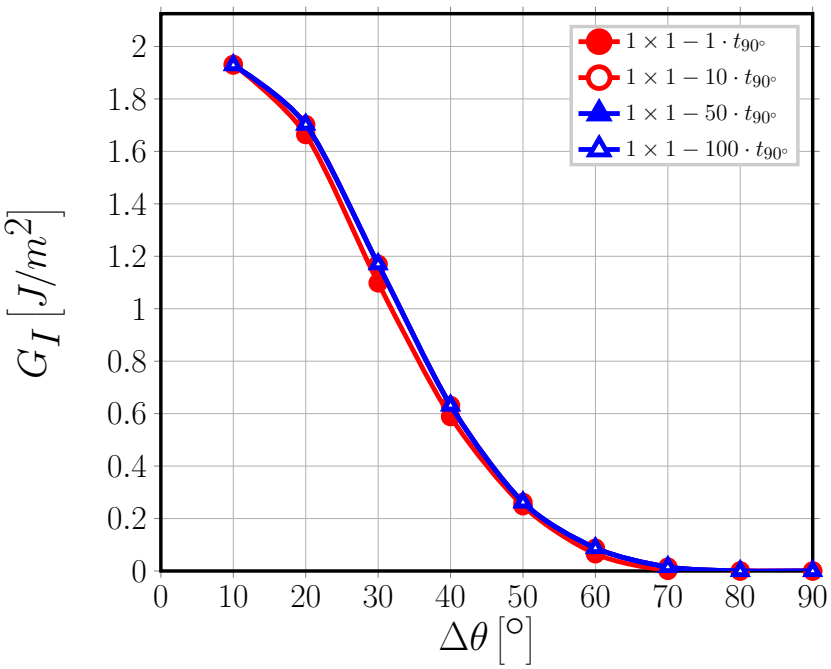

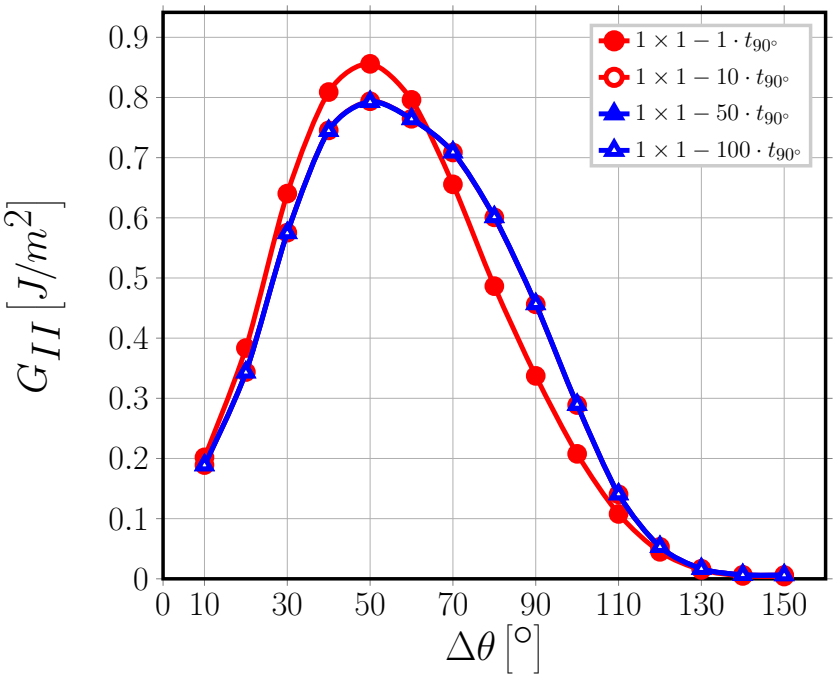

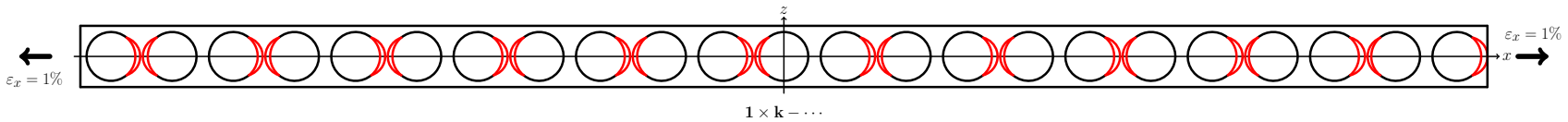

Effect of 0° ply thickness

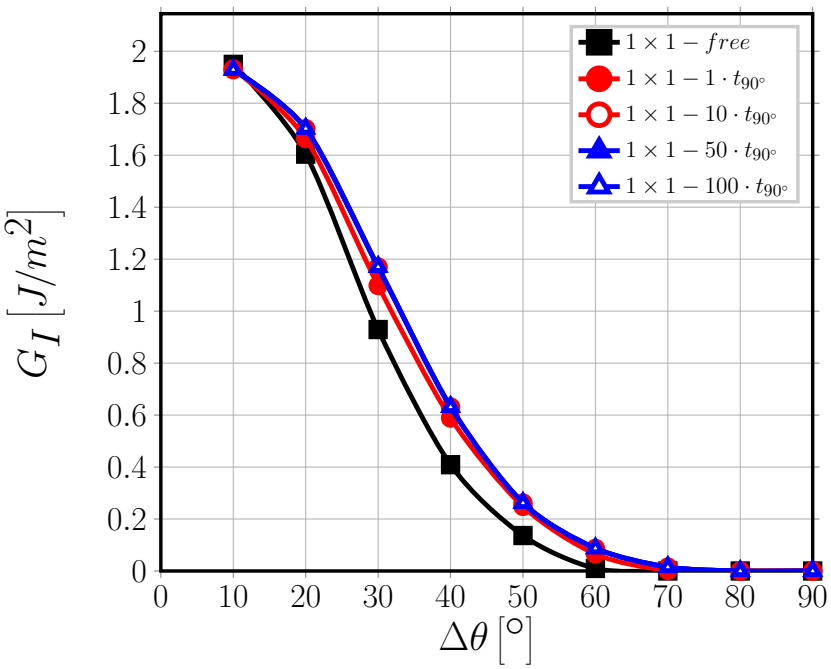

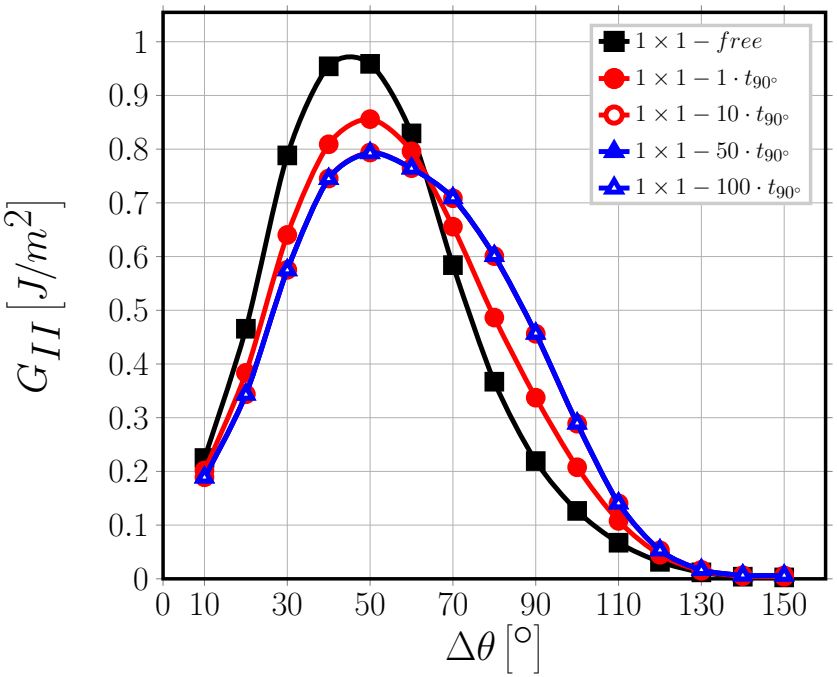

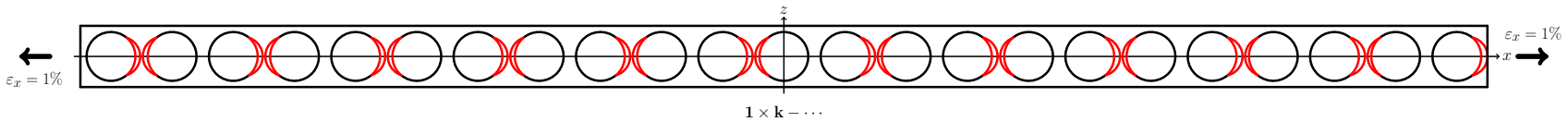

Effect of 0° ply thickness

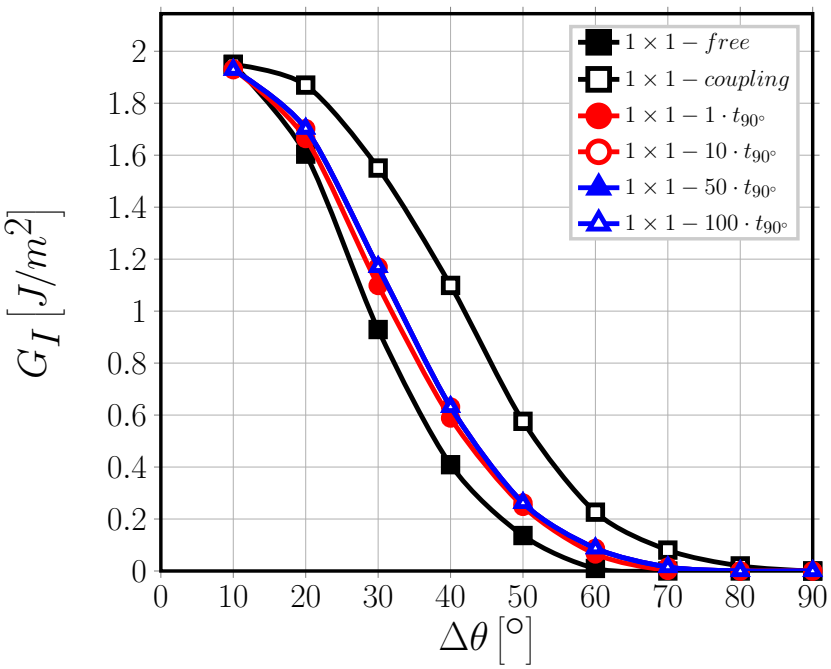

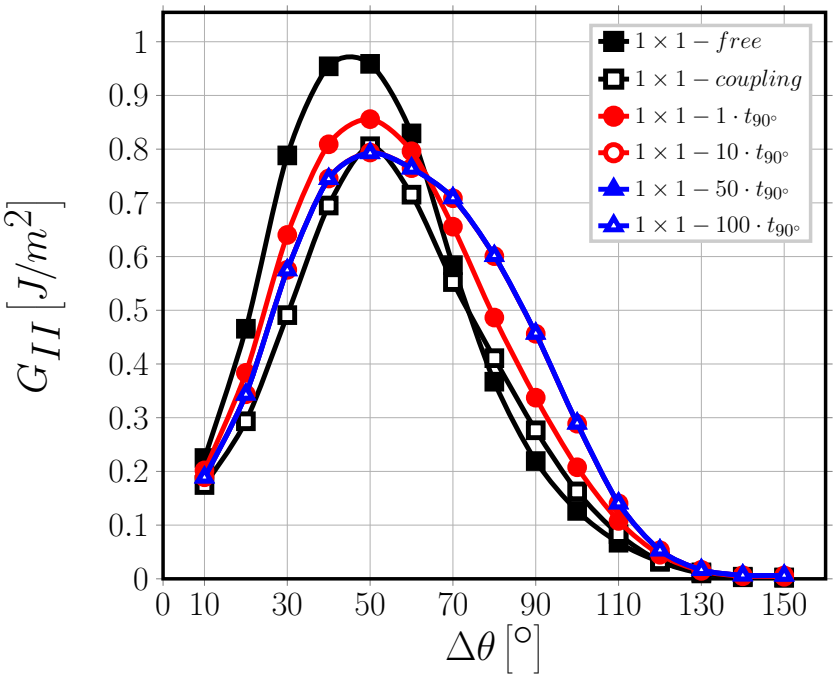

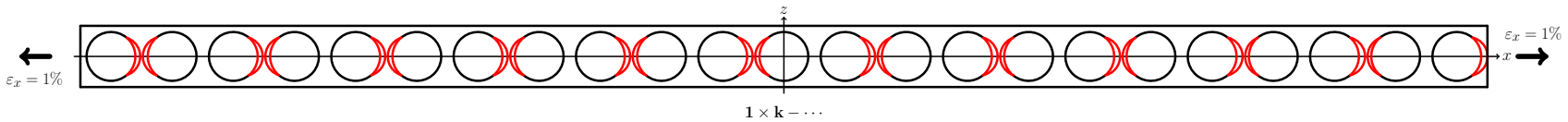

Effect of 0° ply thickness

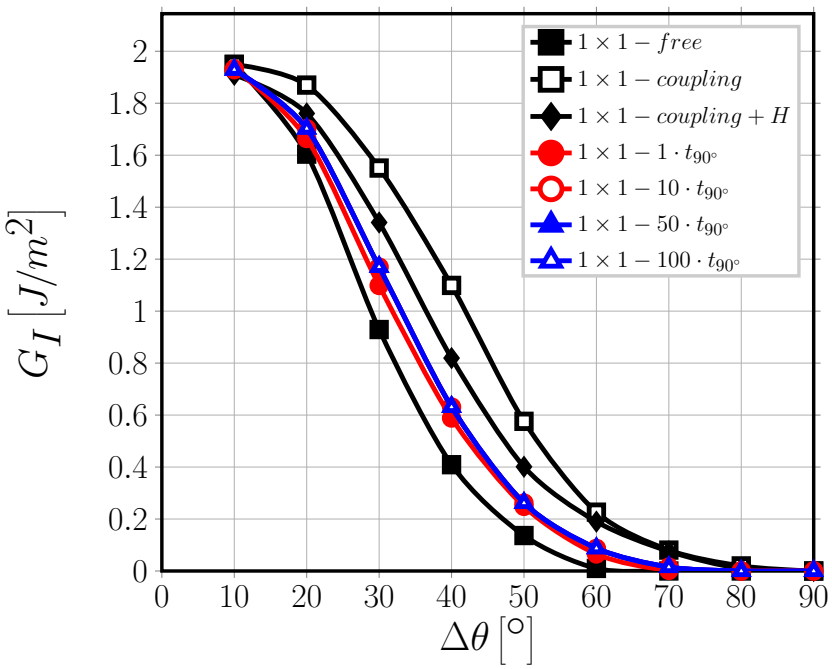

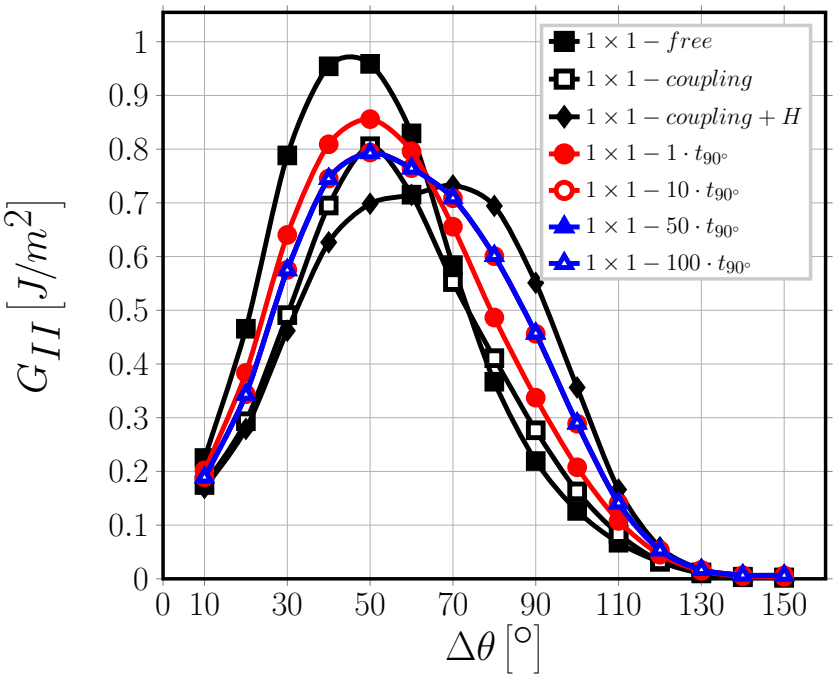

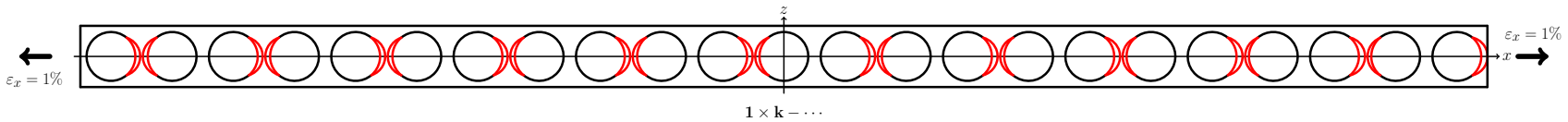

Effect of 90° ply thickness

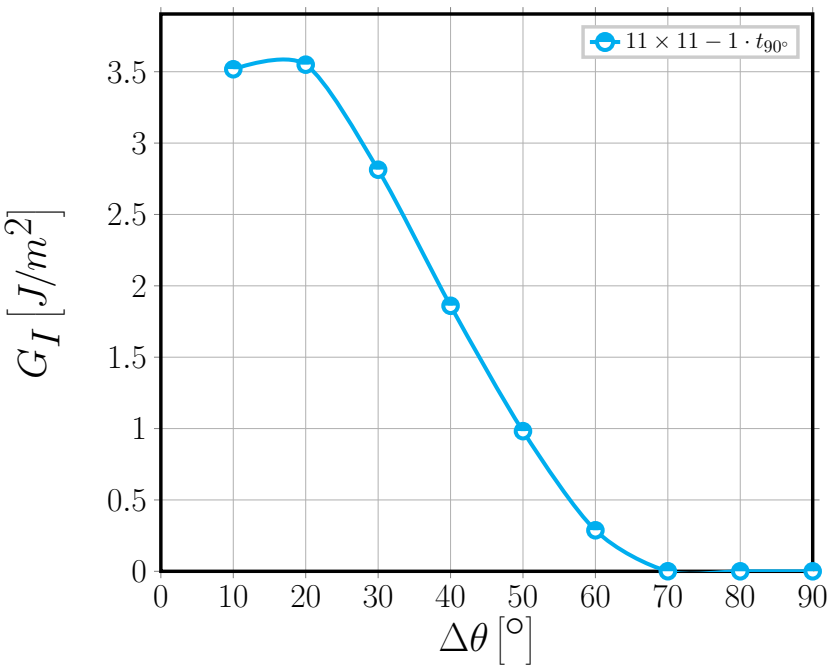

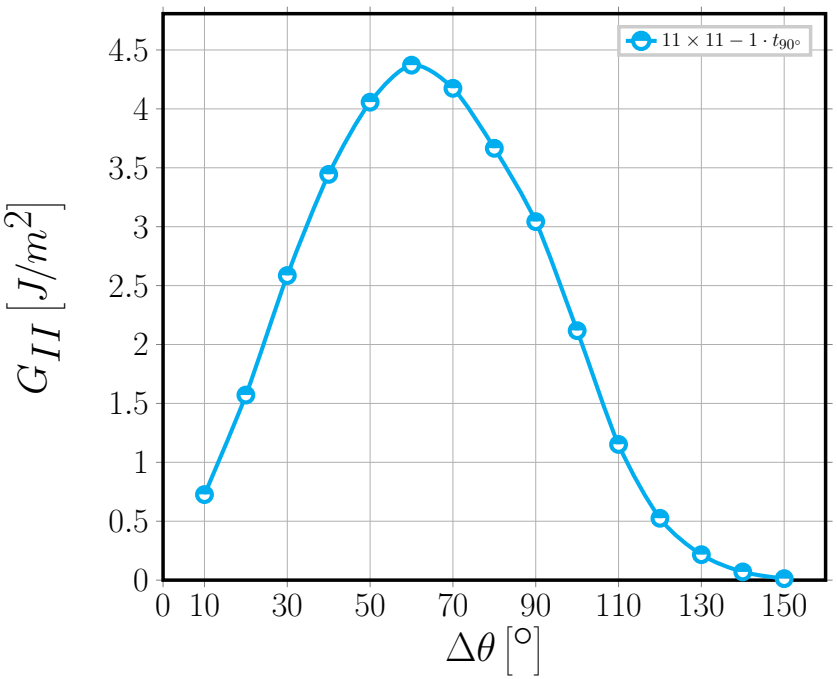

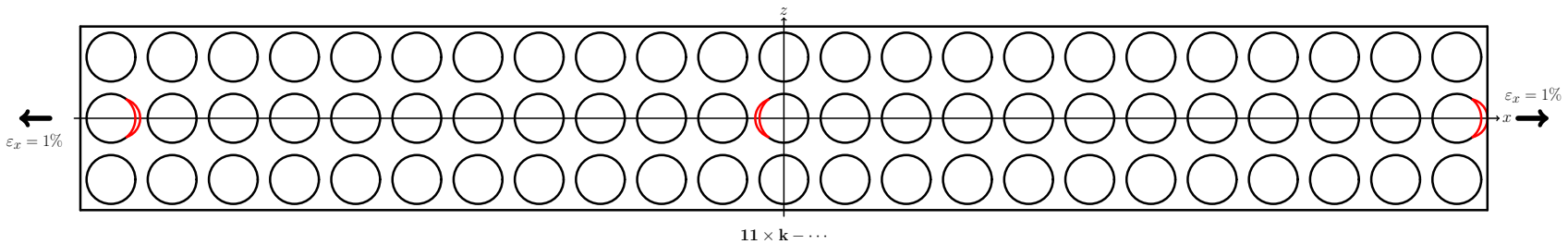

Effect of 90° ply thickness

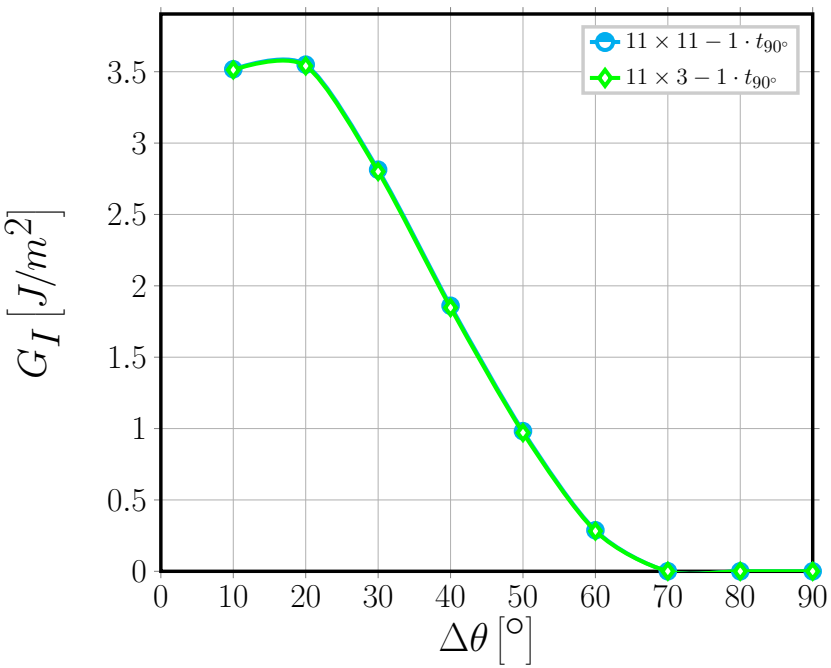

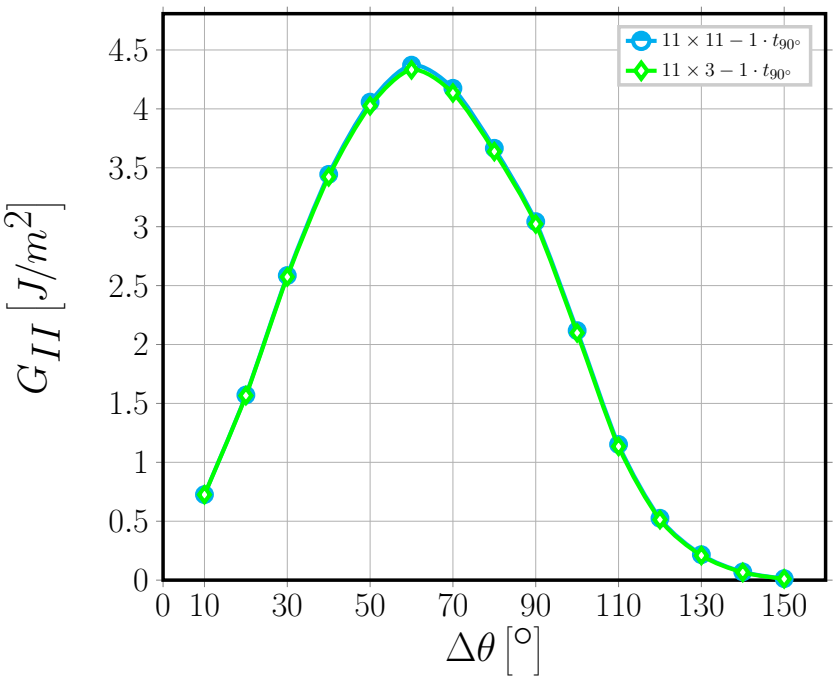

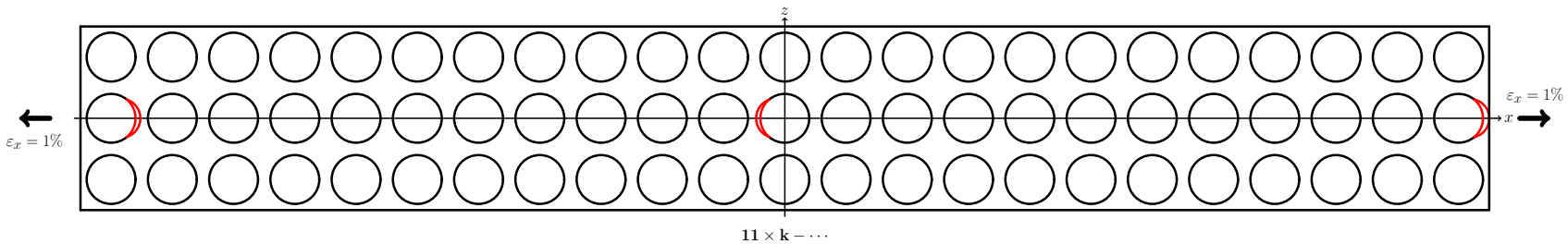

Effect of 90° ply thickness

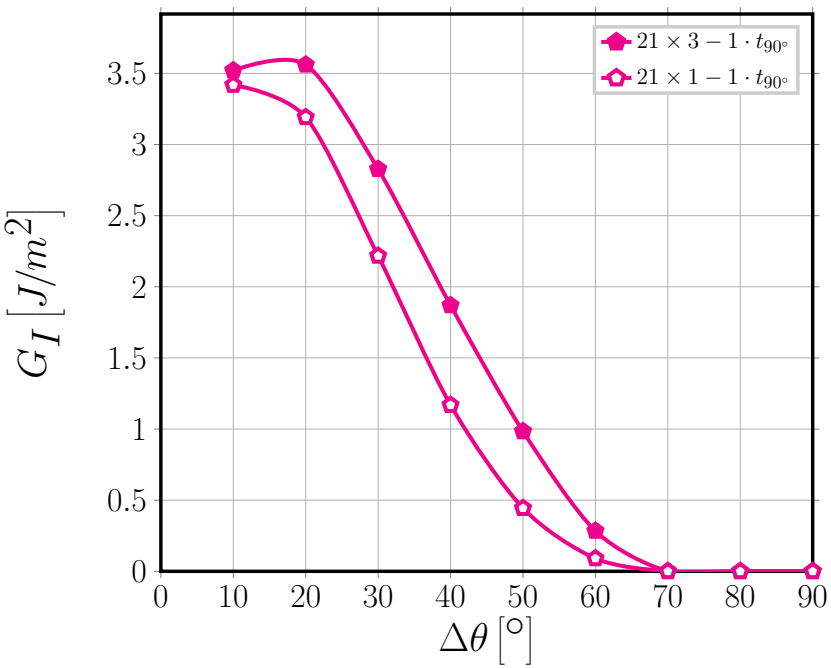

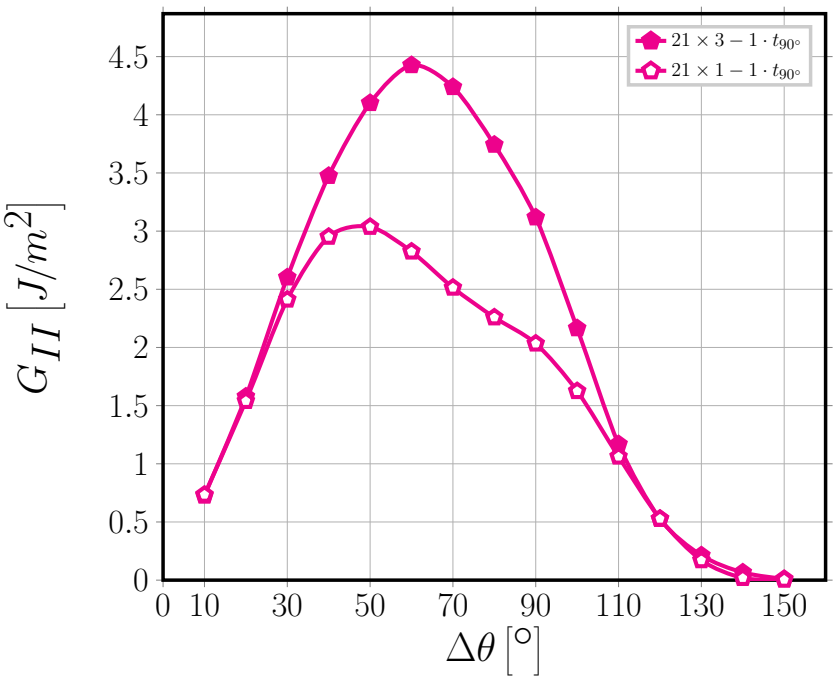

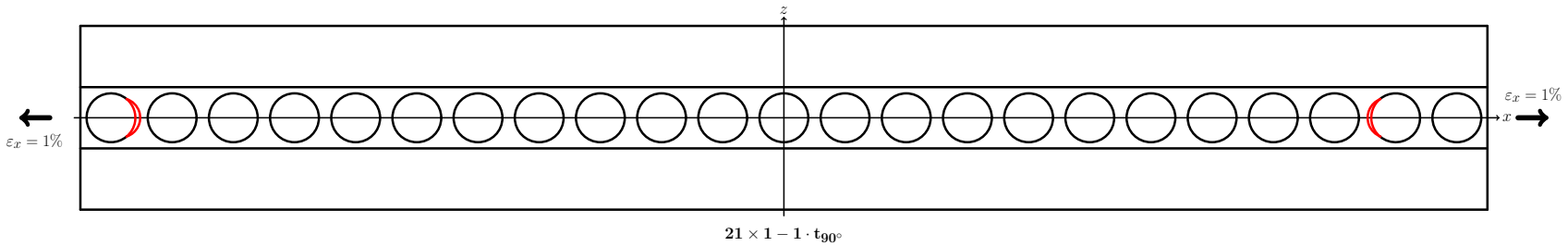

↘ CONCLUSIONS

Conclusions

- ➔ No effect of 90° ply thickness can be observed when t_{90° is at least $\sim 3\varnothing_{fiber}$
- ➔ Only if t_{90° is reduced to $1\varnothing_{fiber}$, ERR is reduced for a given level of applied strain, i.e. debond growth is delayed to higher levels of applied strain ($G \sim \varepsilon^2_{applied}$)
- ➔ No effect of 0° ply thickness can be observed when $t_{0^\circ}/t_{90^\circ} > 1$
- ➔ A small difference can be observed when $t_{0^\circ} = t_{90^\circ}$, due to the smaller bending stiffness of a thinner 0° layer


DOC MASE
UNIVERSITÉ DE LORRAINE
EEIGM
LULEÅ UNIVERSITY OF TECHNOLOGY
Education and Culture
Erasmus Mundus